Shedding Light on the D$_1$-Like Receptors: A Fluorescence-Based Toolbox for Visualization of the D$_1$ and D$_5$ Receptors

Niklas Rosier,[a] Denise Mönnich,[a] Martin Nagl,[a] Hannes Schihada,[b] Alexei Sirbu,[c] Nergis Konar,[c] Irene Reyes-Resina,[d, e] Gemma Navarro,[d, e] Rafael Franco,[d, f] Peter Kolb,[b] Paolo Annibale,[c, g] and Steffen Pockes*[a, h]

Dopamine D$_1$-like receptors are the most abundant type of dopamine receptors in the central nervous system and, even after decades of discovery, still highly interesting for the study of neurological diseases. We herein describe the synthesis of a new set of fluorescent ligands, structurally derived from D$_1$R antagonist SCH-23390 and labeled with two different fluorescent dyes, as tool compounds for the visualization of D$_1$-like receptors. Pharmacological characterization in radioligand binding studies identified UR-NR435 (**25**) as a high-affinity ligand for D$_1$-like receptors (pK_i (D$_1$R) = 8.34, pK_i (D$_5$R) = 7.62) with excellent selectivity towards D$_2$-like receptors. Compound **25** proved to be a neutral antagonist at the D$_1$R and D$_5$R in a G$_s$ heterotrimer dissociation assay, an important feature to avoid receptor internalization and degradation when working with whole cells. The neutral antagonist **25** displayed rapid association and complete dissociation to the D$_1$R in kinetic binding studies using confocal microscopy verifying its applicability for fluorescence microscopy. Moreover, molecular brightness studies determined a single-digit nanomolar binding affinity of the ligand, which was in good agreement with radioligand binding data. For this reason, this fluorescent ligand is a useful tool for a sophisticated characterization of native D$_1$ receptors in a variety of experimental setups.

Introduction

Dopamine (DA, Figure 1) is a catecholaminergic neurotransmitter, which is widely expressed in the central nervous system (CNS), especially in the nigrostriatal, mesolimbic, mesocortical, and tuberoinfundibular systems.[1–3] DA exerts its physiological functions via five G protein-coupled receptors (GPCRs), the dopamine D$_{1-5}$ receptors (D$_{1-5}$R).[4] These five dopamine receptors are divided into two sub-families based on their ability to activate or inhibit the adenylyl cyclase and hence the production of the second messenger cAMP.[5] The D$_1$R and D$_5$R are Gα$_s$-coupled and form the D$_1$-like receptor family, whereas the D$_2$R, D$_3$R, and D$_4$R are Gα$_{i/o}$-coupled and members of the D$_2$-like receptor family.[6,7] Due to the wide expression of dopamine and its receptors in the central and peripheral nervous system they have been the focus of research for many years. Malfunctions of the dopaminergic systems are related to a large number of diseases including schizophrenia, Parkinson's disease (PD), bipolar disorder, depression, restless leg syndrome, hyperprolactinaemia, hypertension, gastroparesis, nausea, and erectile dysfunction.[4,5,8–13] Most of the drugs that are on the market target the D$_2$-like receptors, such as haloperidol, pramipexol, and metoclopramide.[14–16] The only approved drug targeting the D$_1$-like receptors is the peripheral acting partial agonist

[a] Dr. N. Rosier, D. Mönnich, Dr. M. Nagl, Dr. S. Pockes
Institute of Pharmacy
University of Regensburg
Universitätsstraße 31, 93053 Regensburg (Germany)
E-mail: steffen.pockes@ur.de

[b] Dr. H. Schihada, Prof. Dr. P. Kolb
Department of Pharmaceutical Chemistry
University of Marburg
Marbacher Weg 6, 35037 Marburg (Germany)

[c] A. Sirbu, N. Konar, Prof. Dr. P. Annibale
Max Delbrück Center for Molecular Medicine
13125 Berlin (Germany)

[d] Dr. I. Reyes-Resina, Prof. Dr. G. Navarro, Prof. Dr. R. Franco
CiberNed, Network Center for Neurodegenerative Diseases
National Spanish Health Institute Carlos III
Madrid (Spain)

[e] Dr. I. Reyes-Resina, Prof. Dr. G. Navarro
Department Biochemistry and Physiology
School of Pharmacy and Food Sciences
Universitat de Barcelona
Barcelona (Spain)

[f] Prof. Dr. R. Franco
Department of Biochemistry and Molecular Biomedicine
Faculty of Biology, Universitat de Barcelona
Barcelona (Spain)

[g] Prof. Dr. P. Annibale
School of Physics and Astronomy
University of St. Andrews
North Haugh, St. Andrews, Scotland (UK)

[h] Dr. S. Pockes
Department of Medicinal Chemistry
Institute for Therapeutics Discovery and Development
University of Minnesota
Minneapolis, MN 55414 (USA)

[**] A previous version of this manuscript has been deposited on a preprint server (https://doi.org/10.1101/2023.09.25.559386).

Supporting information for this article is available on the WWW under https://doi.org/10.1002/cbic.202300658

ChemBioChem

Research Article
doi.org/10.1002/cbic.202300658

Chemistry Europe
European Chemical
Societies Publishing
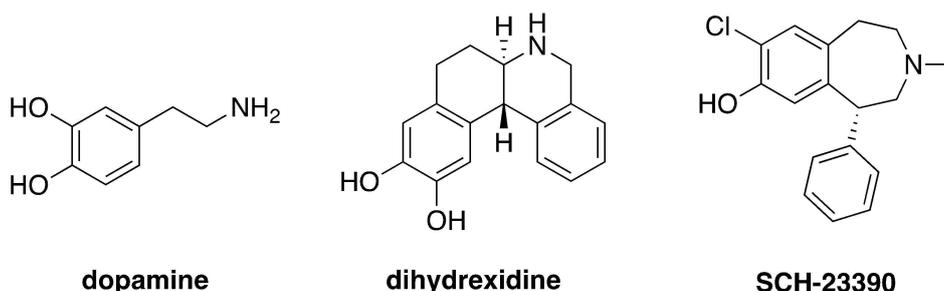
Figure 1. Chemical structures of dopamine, dihydrexidine (D_1R agonist), and SCH-23390 (D_1R/D_5R antagonist).

fenoldopam for the intravenous treatment of hypertension.[17,18] The central active D_1R selective full agonist dihydrexidine (Figure 1) was tested in clinical trials for the treatment of PD but failed due to severe side effects including flushing, hypotension, and tachycardia.[19,20] Despite decades of research, the complex dopaminergic system including the interactions of dopamine receptors with others, such as other dopamine receptors, histamine, NMDA, or adenosine receptors is not fully understood yet and further investigations are needed.[21–24]

Fluorescent ligands represent attractive alternatives to radioligands, for example, to visualize receptors in cells and tissues or for studying the effect of drug-receptor-interactions with advanced biophysical technologies.[25,26] Many fluorescence-based techniques have been developed to study ligand-protein-interactions, including flow cytometry, fluorescence anisotropy, fluorescence polarization as well as resonance energy transfer (RET) based assays.[27–29] Furthermore fluorescence microscopy techniques such as confocal microscopy and total internal reflection fluorescence (TIRF) microscopy are often used for these purposes.[30,31] Traditionally, radiolabeling has been the method of choice to yield labeled ligands for the use as probes in receptor binding assays.[32] In the past decades, fluorescence-based binding assays have become increasingly important and are now almost as present as radiochemical binding assays.[28] The list of advantages and disadvantages of these two methods is relatively balanced. Especially in the areas of safety issues, accessibility, regulatory requirements and cost, fluorescence-based methods can be mentioned as more advantageous. Clear advantages are often seen in the simplicity of implementation and the fact that modern FRET/BRET-based assay systems allow kinetic measurements in real-time.[33,34] In contrast, radioassays are usually very robust, there is no need for receptor modification, access to autoradiography, and high sensitivity to name just a few.[32] For these reasons, both methods will continue to coexist and can be selected to characterize GPCRs and their ligands depending on the respective task. Although FRET/BRET-based assays provide valid results and bring several advantages over, e.g., radioassays, modifications must be made to the GPCR and cell protein of interest. Label-free techniques such as dynamic mass redistribution (DMR), surface plasmon resonance (SPR) and bio-layer interferometry (BLI) are attractive because the isoform of, e.g., the G protein that couples to the receptor of interest doesn't need to be known and genetic modification of the receptor is not required.[35–37] This allows studies under more physiological-like conditions, not least because cellular processes are not impaired by the addition of chemical substances that are often required for signal detection in conventional assays. Although not all processes from label-free readouts leading to the observed signal are yet fully understood and sometimes referred to as "black box" readouts,[38] these technique represents a highly interesting alternative to investigate ligand-receptor interactions.

We herein report the development and validation of a series of six novel fluorescent ligands for D_1-like receptors and their use for binding studies in fluorescence microscopy. Although several fluorescent ligands for the D_1R have previously been published, to our knowledge none of them was tested at the D_5R or has been used for molecular brightness studies.[39–41] The goal of the study is to find useful pharmacological tools that can further help to explore the complex functionalities and interactions of D_1-like receptors.

Results and Discussion

Design rationale

Fluorescent ligands can be considered as an entity of three distinct parts: the ligand scaffold, the linker, and the fluorescent dye. Each of the three parts must be chosen individually based on the intended use of the tool compound.[42–44]

The known D_1R/D_5R antagonist SCH-23390 (Figure 1) was chosen as the structural motif for D_1-like receptors because it displays high affinity at the D_1R and D_5R and a high selectivity within the dopamine receptor family.[45] As a ligand scaffold, an antagonistic partial structure was preferred since agonists can induce receptor internalization and degradation, which could be disadvantageous for binding studies.[42] Structure-activity relationships (SAR) revealed that structural modifications and attachments at the *para*-position of the phenyl group are well tolerated and that a sulfonamide group may be beneficial for binding affinity.[46,47] In accordance with these SAR results, cryo-EM structures of D_1R-G_s complexes bound to an agonistic SCH-23390-derivative, SKF-83959, showed that this position points towards the extracellular space and is not involved in ligand-receptor interaction.[48,49] The solved cryo-EM structures with compound SKF-83959 and the D_1R are shown in Figure S32

ChemBioChem

Research Article
doi.org/10.1002/cbic.202300658

**Chemistry
Europe**
European Chemical
Societies Publishing

(Supporting Information (SI)) and underpin our design rationale. Therefore, this position and chemical moiety were chosen for the attachment of the linker.

Based on previously described D_1R fluorescent ligands, which had the fluorescent dye directly attached to the D_1-like scaffold, two ligands with a short alkylic linker were synthesized.[41] Additionally, fluorescent ligands with longer PEG-based linkers were prepared which should allow the fluorophore to reach outside the binding pocket and therefore, should have reduced impact on the ligand binding. PEG-based linkers are commonly used in fluorescent ligands because they usually don't interact with cell membranes, are chemically stable, and well soluble in water.[50] The connection of the ligand scaffold with the PEG-unit was performed in three steps. First, a short alkylic spacer was attached to the D_1-like scaffold, which was then connected via a peptide coupling reaction to propargylamine. This product was coupled via a copper catalyzed azide alkyne click (CuAAC) reaction[51–53] to a PEG-2 or PEG-3 unit, which was orthogonally functionalized with a primary amine and an azide group (**17a**, **17b**). The additional triazole moiety increases the solubility of the final fluorescent ligands.

The choice of the fluorescent dye is crucial and depends mainly on the intended use of the final fluorescent ligand. Important criteria to consider are spectral properties, quantum yield, solubility, solvatochromic effects, chemical stability, photostability, commercial availability, and an efficient coupling to the ligand scaffold.[42] The 5-TAMRA fluorescent dye was chosen to label the ligands because it is known to yield excellent results in fluorescence microscopy.[34,54,55] Additionally, DY549-P1 from Dyomics was used, as it possesses similar spectral properties as 5-TAMRA. Both dyes are hydrophilic, reducing the risk of unspecific interactions with cell membranes as compared to, for example, BODIPY fluorescent dyes, leading to lower non-specific binding.[56]

Chemistry

The syntheses of the D_1-like scaffold and linkers were performed separately followed by the connection of both parts. The last step in the synthesis of the different fluorescent ligands was always the labeling with a fluorescent dye.

The ligand scaffold was synthesized following the general synthetic route for benzazepines used by Neumeyer et al. and Shen et al. with modifications (Scheme 1).[57,58] In a three-step synthesis 4-nitroacetophenone was transformed into the corresponding epoxide **3** with good yields. Commercially available 4-methoxybenzaldehyde was first chlorinated using sulfurylchloride in acetic acid to afford 3-chloro-4-methoxybenzaldehyde (**4**). A Henry-reaction with nitromethane in acetic acid, followed by a reduction with LiAlH$_4$ in THF afforded the primary amine **6**. The secondary amine **8** was prepared via the introduction of a Boc-protecting group (**7**) and subsequent reduction with LiAlH$_4$. This two-step synthesis provided selectively the mono-methylated amine in high yields. A nucleophilic substitution of the
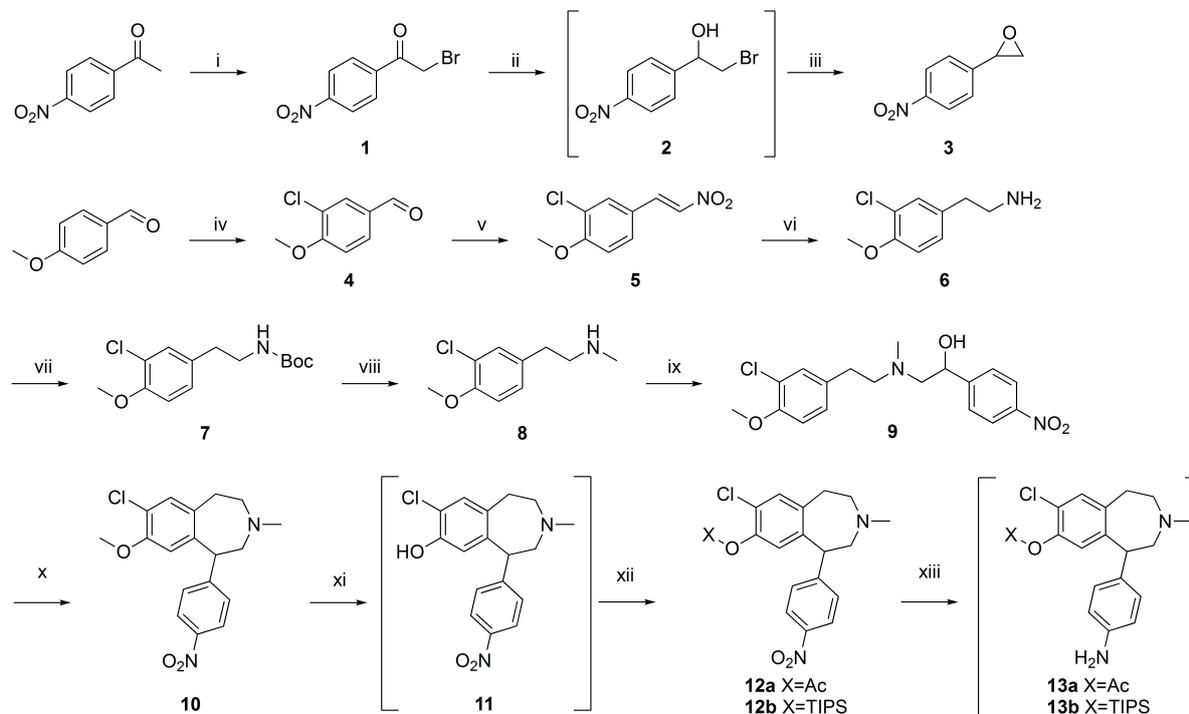
Scheme 1. Synthesis of the ligand scaffolds **13a** and **13b**. Reagents and conditions: i) NBS, pTsOH, DCM, reflux, overnight, 64%; ii) NaBH$_4$, MeOH, rt, 1 h, 66%; iii) K$_2$CO$_3$, THF, reflux, overnight, 87%; iv) SO$_2$Cl$_2$, AcOH, rt, overnight, 86%; v) MeNO$_2$, NH$_4$OAc, AcOH, reflux, 4 h, 68%; vi) LiAlH$_4$, THF, reflux, 3 h, 94%; vii) Boc$_2$O, DCM, rt, overnight, 98%; viii) LiAlH$_4$, THF, reflux, 3 h, 90%; ix) **3**, THF, reflux, overnight, 90%; x) Eaton's reagent, rt, 72 h, 45%; xi) BBr$_3$, DCM, −78°C, overnight, 84%; xii) a) AcCl, NEt$_3$, DCM, rt, overnight, 77%; b) TIPSCl, imidazole, NEt$_3$, DMF, rt, overnight, 90%; xiii) H$_2$, Pd/C, THF/MeOH, rt, overnight, 95%. Compounds **2**, **11**, **13a**, and **13b** were displayed in square brackets, as they were used without further purification and without full analytical characterization.

ChemBioChem

Research Article
doi.org/10.1002/cbic.202300658

Chemistry Europe
European Chemical
Societies Publishing

secondary amine **8** with epoxide **3** in acetonitrile generated product **9** in excellent yields, which was converted to the benzazepine **10** by an acid catalyzed cyclization reaction using Eaton's reagent at room temperature for 72 h. After deprotection with boron tribromide in DCM, the resulting phenol **11** was protected with acetyl chloride or triisopropylsilyl chloride, respectively (**12a**, **12b**). A reduction of the nitro group with hydrogen and catalytical amount of palladium on charcoal in a mixture of MeOH and THF afforded the anilines **13a** and **13b**.

For the introduction of the sulfonylamide moiety two different sulfonyl chlorides (**14a**, **14b**) were required. They were synthesized starting from aliphatic bromides using thiourea and *N*-chlorosuccinimide (Scheme 2A) following the procedure of Yang and Xu et al.[59] The PEG-linkers (**22a**, **22b**) were synthesized starting from the corresponding polyethylene glycols following the reaction protocol published by Iyer et al.[34,60]

Coupling of the sulfonylchlorides **14a** and **14b** with the anilines **13a** and **13b** in the presence of pyridine afforded the structures **18** and **20** (Scheme 2B) in moderate yields. **18** was converted to the primary amine **19** using hydrazine hydrate in ethanol, which simultaneously cleaved the acetyl group affording the free phenol. Purification by preparative HPLC afforded **19** in high purity as the final precursor for coupling to the fluorescent dyes. Ester hydrolysis of **20** under basic conditions and subsequent amide coupling with propargylamide using HATU as a coupling reagent obtained the terminal alkyne **21** in high yields. The triisopropylsilyl protecting group was cleaved as well during this reaction affording the free phenol, which is essential for ligand binding to the D$_1$-like receptors. By using a copper catalyzed alkyne azide click reaction protocol with CuSO$_4$ pentahydrate and ascorbic acid as catalysts[53] **21** was coupled to the PEG linkers. Due to complex purification by preparative HPLC the products (**22a**, **22b**) were isolated in low but sufficient yields for the coupling with the fluorescent dyes.

All three precursors were labelled with both fluorescent dyes (5-TAMRA-NHS ester and DY549-P1-NHS ester) in DMF with an excess of NEt$_3$ as a base (Scheme 3).[61] Purification by preparative HPLC afforded the final fluorescent ligands (**23**–**28**) in moderate to good yields, great purity, and stability (Figures S1–S6; SI).

Pharmacological Characterization

In order to pharmacologically characterize the new set of fluorescent ligands, we first determined their D$_1$-like receptor affinity and picked the best compounds to test for selectivity
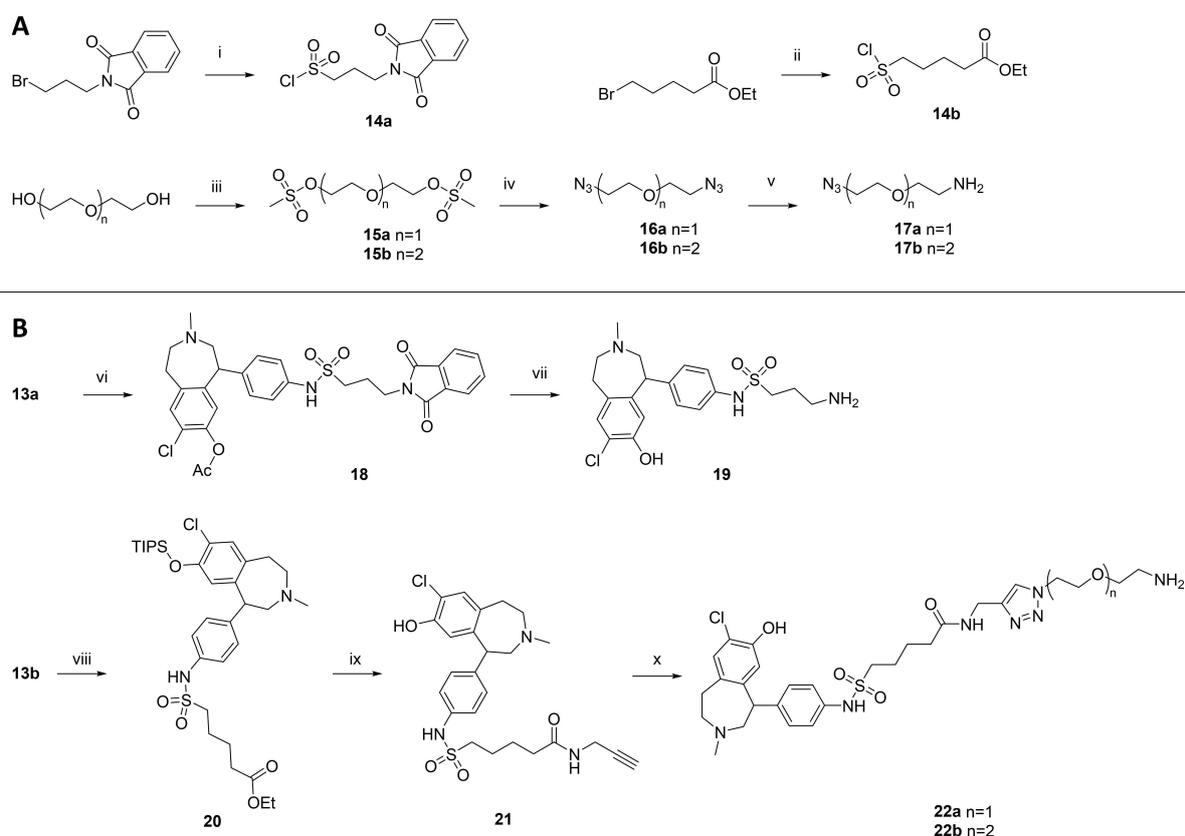
Scheme 2. Synthesis of the sulfonylchlorides and linkers (**A**) and preparation of the final precursors (**B**). Reagents and conditions: i) 1.) thiourea, EtOH, 1 h, reflux, 2.) NCS, MeCN, 2 N HCl, 20 min, 5 °C, 89 %; ii) 1. thiourea, EtOH, overnight, reflux, 2. NCS, MeCN, 2 N HCl, 30 min 5 °C, 87 %; iii) MsCl, NEt$_3$, DCM, rt, overnight, 96 %; iv) NaN$_3$, DMF/EtOH, reflux, overnight, 99 %; v) PPh$_3$, EtOAc/THF/1 N HCl, rt, overnight, 69 %; vi) **14a**, pyridine, CHCl$_3$, 50 °C, overnight, 62 %; vii) hydrazine, EtOH, reflux, overnight, 23 %; viii) **14b**, pyridine, CHCl$_3$, 50 °C, overnight, 56 %; ix) 1. LiOH, H$_2$O/THF, rt, overnight, 2. propargylamine, HATU, DIPEA, DMF, rt, overnight, 92 %; x) **17a/17b**, CuSO$_4$, ascorbic acid, DCM/MeOH, rt, 72 h, 14 %.
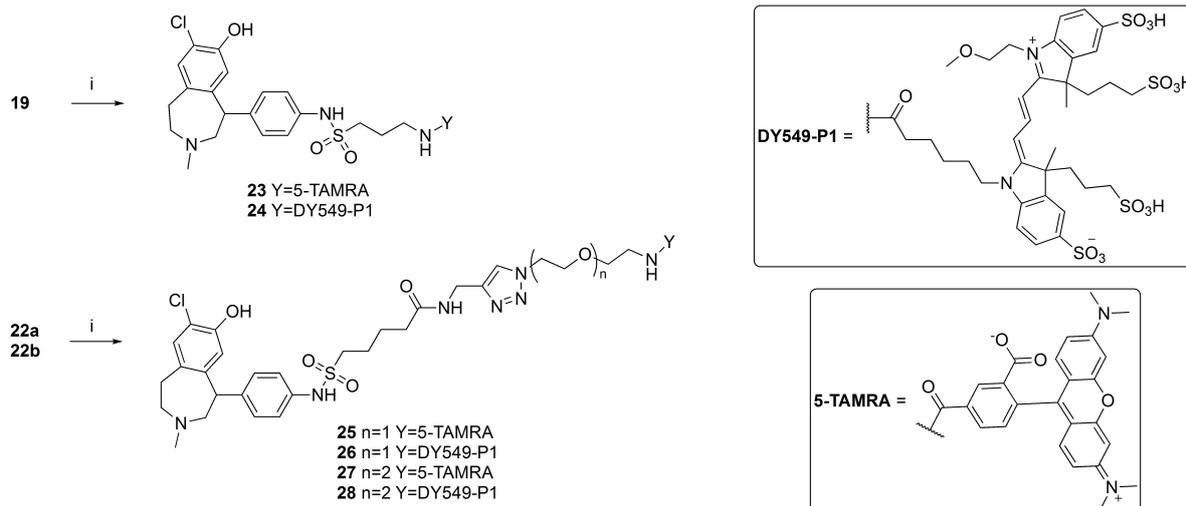
Scheme 3. Synthesis of the fluorescent ligands **23–28**. Reagents and conditions: i) fluorescent dye NHS-ester, NEt$_3$, DMF, 3 h, rt, 39–89%. Full structures of compounds **23–28** are displayed in the SI.

within the dopamine receptor family. Therefore, all compounds were initially tested in radioligand competition binding assays at the wild type D$_1$R (Figure 2A). Here, the fluorescent ligands **24**, **25**, and **27** showed the highest affinities, with the two TAMRA derivatives **25** (pK_i (D$_1$R) = 8.34, Table 1) and **27** (pK_i (D$_1$R) = 8.02, Table 1) showing single-digit nanomolar affinities.

Since the PEG-containing compounds **25–28** were able to show significantly better properties in terms of solubility, further competition experiments were performed with the same compounds at the D$_5$R (Figure 2B). In all cases, reduced affinity values of about 0.4-0.8 logarithmic units were found. Again, the best results were obtained with **25** (pK_i (D$_5$R) = 7.62, Table 1)
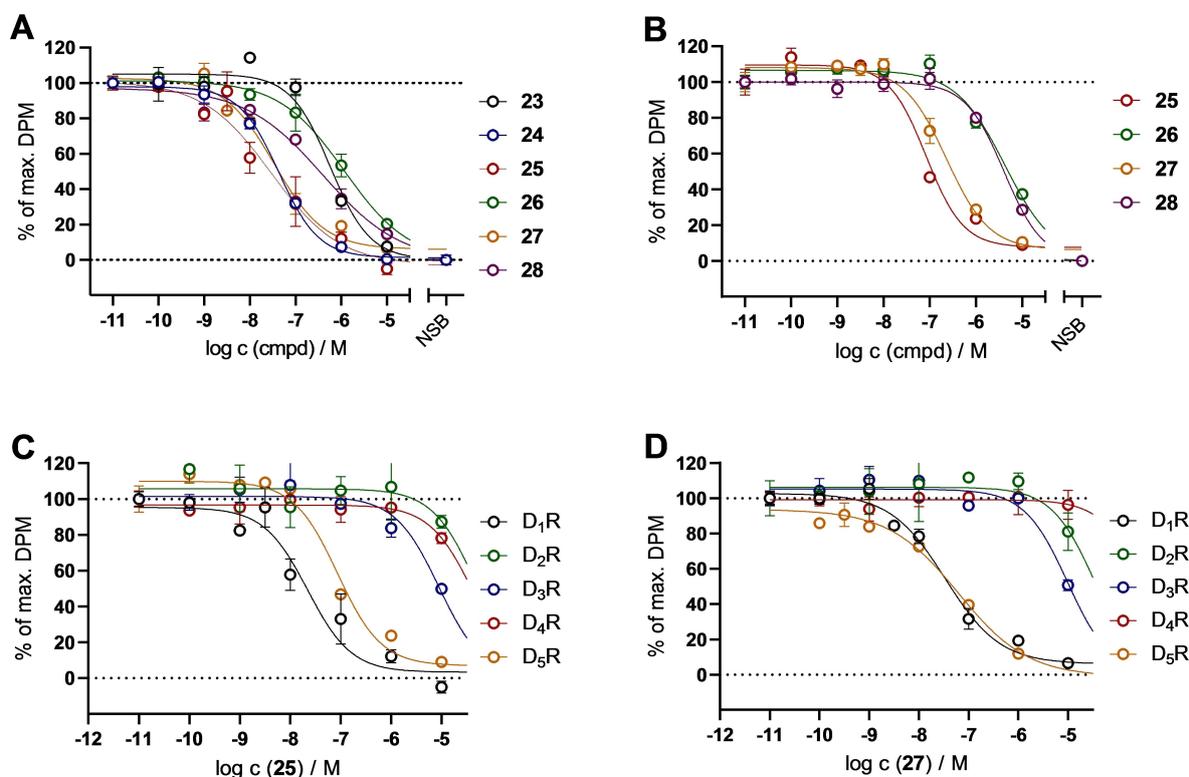
Figure 2. Competition binding curves from radioligand binding experiments at the D$_1$R (**A**) and D$_5$R (**B**) homogenates performed with compounds **23–28** and the respective radioligands (cf. Table 1 footnotes). Competition binding curves of **25** (**C**) and **27** (**D**) at the D$_{1-5}$R homogenates. Graphs represent the means from three independent experiments each performed in triplicates. Data were analyzed by nonlinear regression and were best fitted to sigmoidal concentration-response curves.
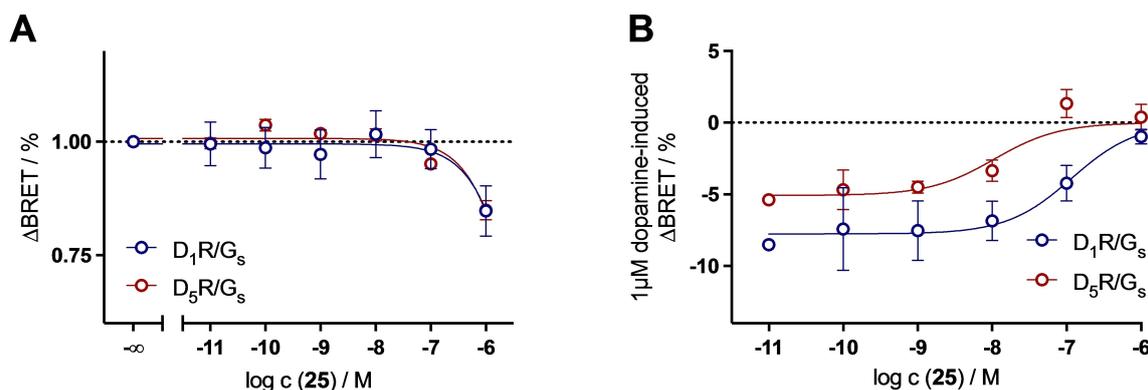
Figure 3. Concentration-response curves (CRCs) for G_s activation of **25** in the absence (**A**) and presence (**B**) of 1 μM dopamine in HEK293 A cells transiently expressing the G_s BRET sensor along with the wild-type D_1R or D_5R. Graphs represent the means of three independent experiments each performed in duplicates. Data were analyzed by nonlinear regression and were best fitted to sigmoidal concentration-response curves.

Table 1. Binding data of **23–28** at the dopamine receptors.									
compound	Radioligand competition binding[a]								
	pK_i								
	$D_1R^{[b]}$	N	$D_{2long}R^{[c]}$	N	$D_3R^{[d]}$	N	$D_4R^{[e]}$	N	$D_5R^{[f]}$	N
23	6.40 ± 0.39	3	n.d.	–	n.d.	–	n.d.	–	n.d.	–
24	7.99 ± 0.18	3	n.d.	–	n.d.	–	n.d.	–	n.d.	–
25	8.34 ± 0.21	3	<5	3	5.67 ± 0.06	3	<5	3	7.62 ± 0.03	3
26	6.54 ± 0.23	3	n.d.	–	n.d.	–	n.d.	–	6.03 ± 0.12	3
27	8.02 ± 0.14	3	<5	3	5.57 ± 0.03	3	<5	3	7.65 ± 0.14	3
28	6.85 ± 0.07	3	n.d.	–	n.d.	–	n.d.	–	6.06 ± 0.10	3

[a] Competition binding assay at HEK293T_CRE Luc 2P D_1R homogenates, HEK293T_CRE Luc 2P $D_{2long}R$ homogenates, HEK293T_CRE Luc 2P D_3R homogenates, HEK293T_CRE Luc 2P D_4R homogenates, or HEK293T_CRE Luc 2P D_5R homogenates. [b] Displacement of 1 nM [³H]SCH-23390 ($K_d = 0.4$ nM). [c] Displacement of 0.05 nM [³H]N-Methylspiperone ($K_d = 0.015$ nM). [d] Displacement of 0.05 nM [³H]N-Methylspiperone ($K_d = 0.026$ nM). [e] Displacement of 0.1 nM [³H]N-Methylspiperone ($K_d = 0.078$ nM). [f] Displacement of 1 nM [³H]SCH-23390 ($K_d = 0.4$ nM). Data shown are mean values ± SEM of N experiments, each performed in triplicates. Data were analyzed by nonlinear regression and were best fitted to sigmoidal concentration-response curves. Competition binding curves are shown in Figure 2.

and **27** (pK_i (D_5R) = 7.65, Table 1). Both compounds were subsequently tested at the $D_{2long}R$, D_3R, and D_4R, and only weak binding to the D_2-like receptors was detected, representing a great selectivity profile over D_2-like receptors for **25** and **27** (at least 1,000-fold for D_1R and at least 500-fold for D_5R). Because of the highest affinity and selectivity, **25** seemed to be the most promising ligand to be used as a fluorescent tracer in microscopy studies. For this purpose, knowing the ligand's mode of action is of great importance since agonists can alter the results of binding studies by inducing receptor internalization and degradation. Therefore, we confirmed the antagonistic behavior of **25** in a BRET-based G_s heterotrimer dissociation assay (G_s-CASE) (Figure 3; Table 2).[62] In the agonist mode, only at high concentrations of 1 μM a slight decrease could be observed, which is most likely due to optical interference of **25** with the BRET components of G_s-CASE as observed in an earlier study with a 5-TAMRA-labeled histamine H_3 receptor ligand (Figure 3A).[34] In contrast, **25** reduced already at lower concentration the 1 μM dopamine-induced BRET response (pK_b (D_1R) = 7.29, pK_b (D_5R) = 9.48; Table 2), indicating that it acts as a neutral antagonist at both, D_1 and D_5 receptors. Concentration-

Table 2. Functional data of **25** at the D_1R and D_5R.				
compound	$G\alpha_s$ activation[a]			
	pK_b			
	$D_1R^{[b]}$	N	$D_5R^{[c]}$	N
25	7.52 ± 0.09	3	9.60 ± 0.16	3

[a] Competition binding experiment at HEK293 cells expressing the G_s BRET sensor with the wild type D_1R or D_5R. [b] Inhibition of dopamine-induced (c = 1 μM, EC_{50} = 393 nM, Figure S7, SI) G_s activation. [c] Inhibition of dopamine-induced (c = 1 μM, EC_{50} = 26 nM, Figure S7, SI) G_s activation. Data shown are mean values ± SEM of N experiments, each performed in duplicates. Data were analyzed by nonlinear regression and were best fitted to sigmoidal concentration-response curves. Competition binding curves are shown in Figure 3.

response curves of dopamine-induced G_s activation at the D_1R and D_5R are shown in Figure S7 (SI).
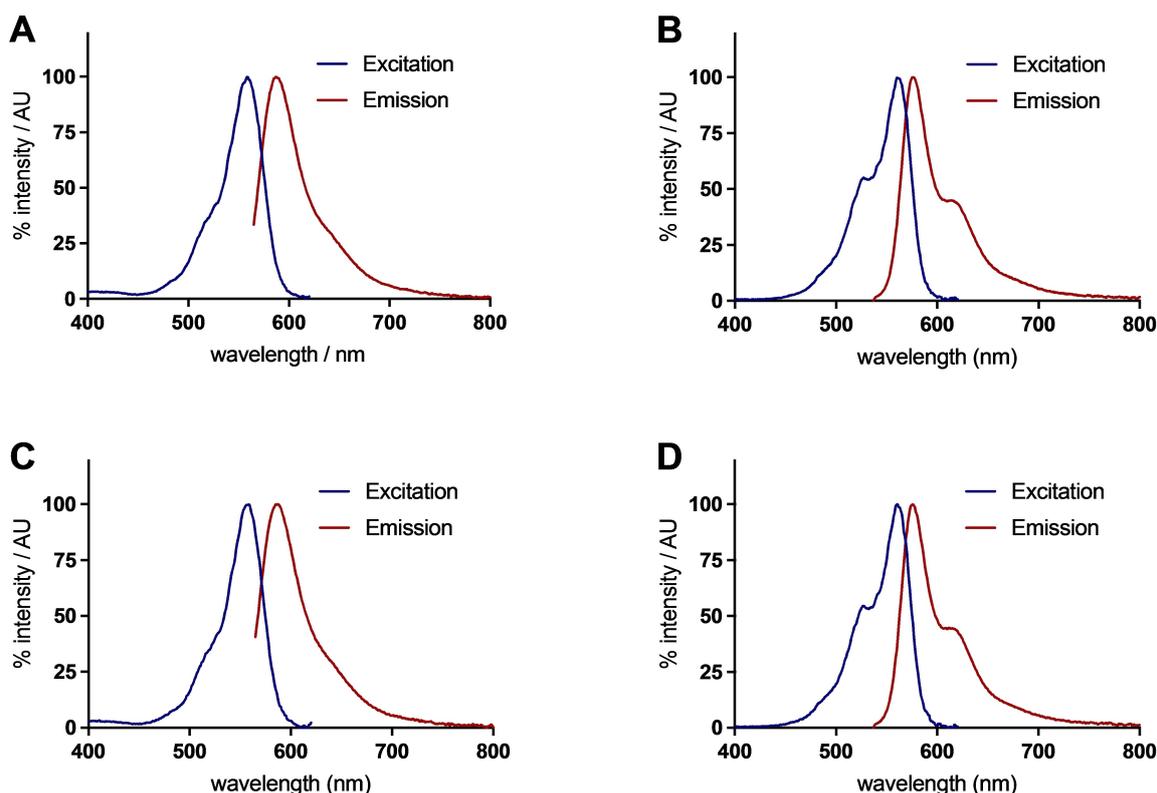
Figure 4. Excitation and emission spectra of **25** (**A**), **26** (**B**), **27** (**C**), and **28** (**D**) recorded in PBS buffer containing 1% of BSA. The excitation wavelength for the emission spectra was 555 nm (**25**, **27**) or 527 nm (**26**, **28**). The emission wavelength collected during the excitation scan was 630 nm.

Fluorescence Properties

The fluorescence properties are usually not heavily affected by the addition of a ligand scaffold, if the fluorophore is chemically not changed, as it's the case for the 5-TAMRA and DY549-P1 dye. Nevertheless, the absorption and emission spectra and the quantum yield should be determined for new fluorescent ligands. The knowledge of the excitation and emission spectra and a high quantum yield are essential for their use in pharmacological assays and fluorescence microscopy. The emission and excitation spectra of **25**–**28** were recorded in PBS buffer containing 1% of BSA (Figure 4). The excitation and emission maxima are presented in Table 3.

The quantum yield of the compounds was determined in PBS buffer containing 1% BSA for all four compounds and additionally in PBS buffer for compounds **25** and **27** (Table 3) following a previously published protocol.[63] The 5-TAMRA-labeled compounds **25** and **27** have a higher quantum yield of approximately 36% in PBS buffer compared to the DY549-P1-labeled ligands (**26** and **28**; approx. 19%). Furthermore, it was observed that the addition of 1% BSA led to a decrease in the quantum yield of the 5-TAMRA-labeled fluorescent ligands, but still with a satisfactory quantum yield of approx. 30%. Based on these results all four ligands, but especially **25** and **27**, should be suitable for the use in fluorescence microscopy.

Microscopy

In order to test the suitability of **25** for laser scanning confocal microscopy (LSCM) and to visualize the binding of **25** to the D_1R, HEK-293T cells were transiently transfected with the D_1R C-terminally tagged with YFP. 48 hours after transfection confocal microscopy images were recorded (Figure S8, SI). After addition of 50 nM of **25** a rapid accumulation of fluorescence at the cell surface was observed. This is caused by the fast association of **25** to the D_1R expressed on the cell membrane reaching saturation binding in less than one minute. Based on the fluorescence intensity of individual cells, a time-dependent association curve could be obtained illustrating the fast binding of **25** to the D_1R followed by a constant dissociation of **25** from the receptor after addition of 50 μM SCH-23390 (1,000-fold excess) (Figure 5). Based on the association and dissociation

Table 3. Fluorescence properties of compounds **25**–**28**.			
compound	$\lambda_{exc,max}/\lambda_{em,max}$ (nm)	Φ (%)[a]	
		PBS	PBS + 1% BSA
25	559/586	36.77 ± 0.41	29.47 ± 0.35
26	561/575	n.d.	19.06 ± 0.26
27	559/585	36.52 ± 0.44	30.77 ± 0.43
28	560/574	n.d.	18.00 ± 0.33
[a] Data shown are mean values ± SEM of three different slit adjustments (exc./em.): 5/5 nm, 5/10 nm, 10/10 nm.			
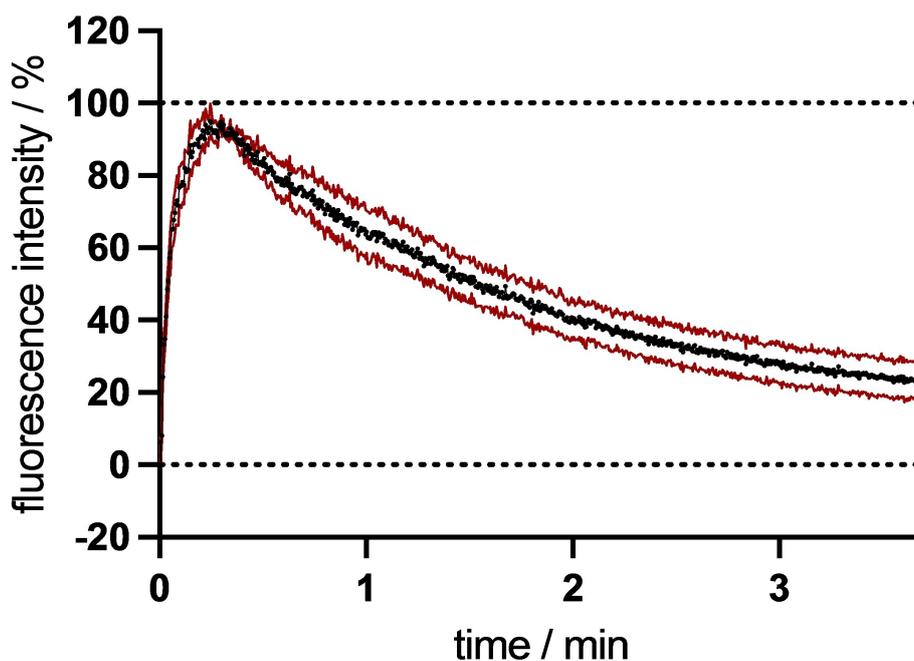
Figure 5. Binding kinetics of **25** at the hD$_1$R in whole HEK-293T cells using LSCM. The graph shows association of **25** (c = 50 nM) to the receptor and dissociation of **25** induced by addition of SCH-23390 (c = 50 µM, 1,000-fold excess, after 15 seconds) from a representative experiment. Data represent mean ± SEM of four independent cells of one experiment.

rates a kinetic pK_d value of 8.07 was calculated (Table 4). These results demonstrate the suitability of **25** for the use in fluorescence microscopy as a labeling agent to visualize the D$_1$R in live cells.

Molecular Brightness

To further characterize the ligand's binding affinity in intact living cells we employed molecular brightness to calculate the number of receptors decorated by the ligand on the basal membrane of cells, for varying ligand concentrations.[64] In order to reference the fraction of ligand-receptor complexes to the total amount of receptors expressed, we transfected HEK293-AD cells with D$_1$R C-terminally tagged with the photostable fluorescent protein mNeonGreen (D$_1$R-mNeonGreen). Cells were incubated with increasing concentrations of **25** and after reaching equilibrium, the ligand was washed out and the cell's basal membranes were imaged over time in the two spectral channels (GFP /receptor and TAMRA/ligand) using a confocal microscope (Figure 6A). From the obtained movies the average number of emitters within the confocal excitation volume was calculated based on the fluctuation of the fluorescence photon counts within each pixel (see methods) and plotted against each other. A linear regression was fitted to the data points and the slope calculated (Figure 6B). A slope of 1 signifies a 1:1 ratio in the number of GFPs and TAMRAs and with this a full occupancy of the receptor by the ligand. Slopes between 0 and 1 represent partial occupancy. Plotting obtained slopes versus logarithmic expression of ligand concentration returns a sigmoid concentration response curve and yields a pK_d of 8.92 ± 0.13, that matches well the results obtained by radioligand binding (Figure 6C).

Table 4. Kinetic binding constants of **25** at the hD$_1$R in confocal microscopy.					
cmpd	confocal microscopy				
	k_{obs}^a (min^{-1})	τ_{ass}^b (min)	k_{off}^c (min^{-1})	τ_{diss}^d (min)	k_{on}^e (min^{-1} nM^{-1})	pK_d (kin)^f
25	5.24 ± 0.43	0.21 ± 0.03	0.76 ± 0.16	1.76 ± 0.88	0.09 ± 0.01	8.07 ± 0.01

[a] 17 cells from four independent experiments were analyzed. Data represent mean values ± SEM. Experiments were performed at HEK293T cells transiently expressing the hD$_1$R. [b] Data represent mean values ± CI (95%). Association time constant: $\tau_{ass} = 1/k_{obs}$. [c] Five cells from one experiment were analyzed. Data represent mean values ± SEM. Experiments were performed at HEK293T cells transiently expressing the hD$_1$R. [d] Data represent mean values ± CI (95%). Dissociation time constant: $\tau_{ass} = 1/k_{off}$. [e] Association rate constant: $k_{on} = (k_{obs} - k_{off})/c$ (**25**). Indicated errors were calculated according to the Gaussian law of error propagation. [f] K_d (kin) = k_{off}/k_{on}; pK_d (kin) = $-\log K_d$ (kin). Indicated errors were calculated according to the Gaussian law of error propagation.
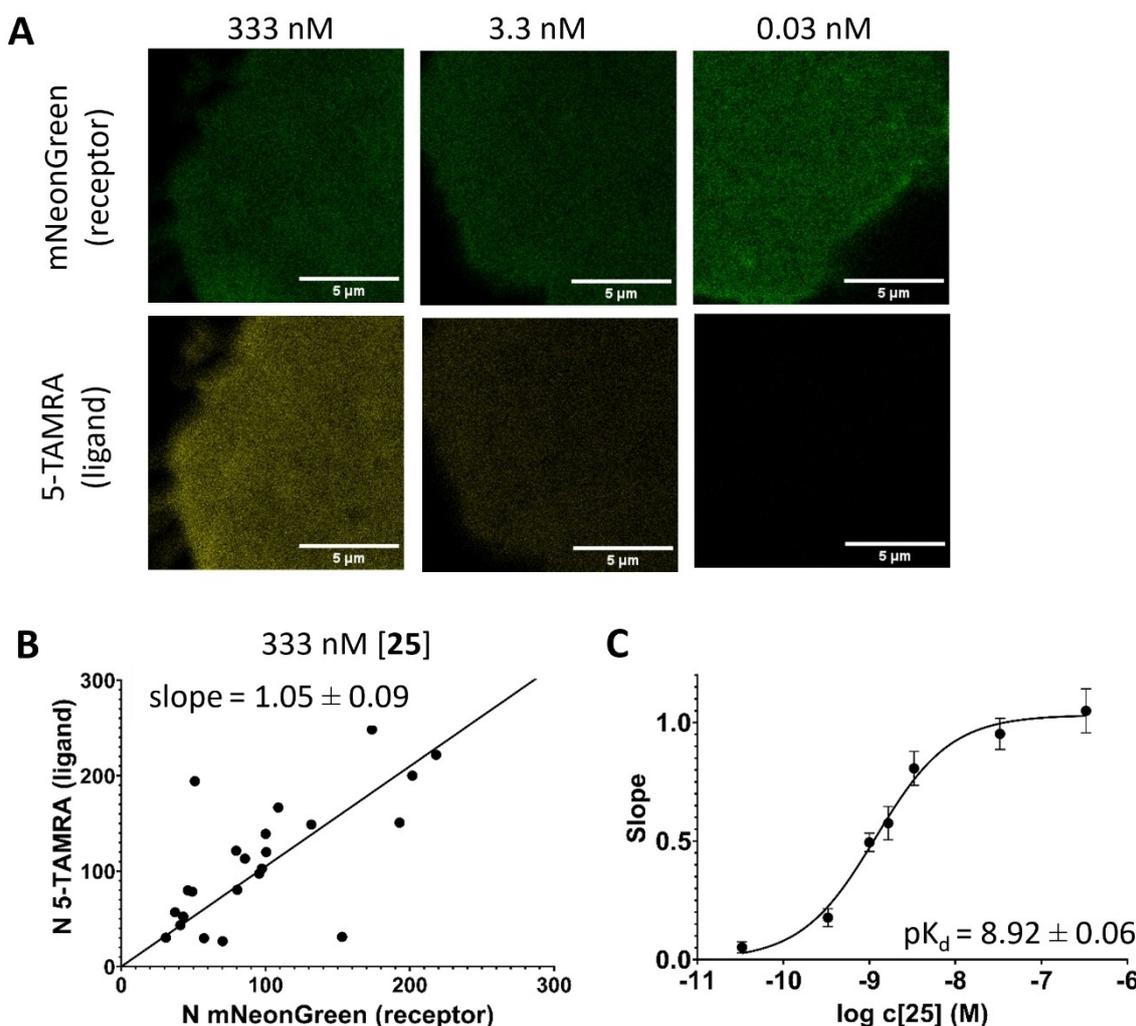
Figure 6. Association of **25** to the hD$_1$R using molecular brightness analysis. Basolateral membranes of HEK-293AD cells transiently expressing hD$_1$R-mNeonGreen and preincubated with indicated amount of **25** (**A**); calculated numbers of emitters for 5-TAMRA and mNeonGreen channels, and the corresponding linear regression fit (mean ± SEM; n = 23 cells from 3 independent experiments) (**B**), slopes obtained from linear fits plotted against log concentrations of **25** with the corresponding non-linear fit and pK$_d$ value (mean ± SEM; n = at least 20 cells from 3 independent experiments for each datapoint) (**C**).

Conclusions

A set of six different fluorescent ligands containing linkers of different lengths and chemical compositions and two different fluorescent dyes were designed and synthesized. The known D$_1$R/D$_5$R antagonistic SCH-23390 was used as a D$_1$-like scaffold for the fluorescent ligands. Two fluorescent dyes, 5-TAMRA and DY549-P1, were chosen because of their proposed suitability as a fluorescent tracer for microscopy studies. After the successful synthesis and purification of the ligands, their fluorescent and pharmacological properties were determined. Radioligand binding studies were performed revealing **25** and **27** as D$_1$-like receptor selective fluorescent ligands with binding affinity in the low nanomolar range. Compound **25**, equipped with the medium-length hydrophilic PEG linker and 5-TAMRA as dye, showed the best overall results regarding affinity, selectivity, quantum yield and was used as an exemplary compound to determine its mode of action. A G protein biosensor assay

confirmed the expected neutral antagonism of **25**. Furthermore, **25** was used successfully to label D$_1$Rs in live cells for LSCM demonstrating its suitability for fluorescence microscopy. In molecular brightness studies, the ligand's binding affinity could be determined in a range that was in good agreement with radioligand binding data and a full occupancy of the receptor by the ligand. Overall, the set of fluorescent ligands, especially **25**, represent a versatile tool for different experimental setups for further investigations at the D$_1$-like receptors.

Experimental Section

Chemistry

Commercially available chemicals and solvents were purchased from standard commercial suppliers (Merck (Darmstadt, Germany), Sigma-Aldrich (Munich, Germany), Acros Organics (Geel, Belgium), Alfa Aesar (Karlsruhe, Germany), abcr (Karlsruhe, Germany) or TCI

ChemBioChem

Research Article
doi.org/10.1002/cbic.202300658

Chemistry Europe
European Chemical
Societies Publishing

Europe (Zwijndrecht, Belgium) and were used as received. All solvents were of analytical grade. The fluorescent dye 5-TAMRA NHS ester was purchased from Lumiprobe (Hannover, Germany). The fluorescent dye DY549-P1 was purchased from Dyomics GmbH (Jena, Germany). Deuterated solvents for nuclear magnetic resonance (^{1}H NMR and ^{13}C NMR) spectra were purchased from Deutero GmbH (Kastellaun, Germany). All reactions carried out with dry solvents were accomplished in dry flasks under nitrogen or argon atmosphere. For the preparation of buffers, HPLC eluents, and stock solutions millipore water was used. Column chromatography was accomplished using Merck silica gel Geduran 60 (0.063–0.200 mm). Flash chromatography was performed using an Agilent Technologies 971-FP Flash Purification System (Agilent Technologies, Santa Clara, CA) with SI-HP 30 μm puriFlash columns from Interchim (Montlucon, France). The reactions were monitored by thin layer chromatography (TLC) on Merck silica gel 60 F254 aluminium sheets and spots were visualized under UV light at 254 nm, by potassium permanganate or ninhydrin staining. Lyophilization was done with a Christ alpha 2–4 LD equipped with a vacuubrand RZ 6 rotary vane vacuum pump. Nuclear magnetic resonance (^{1}H NMR and ^{13}C NMR) spectra were recorded on a Bruker (Karlsruhe, Germany) Avance 300 (^{1}H: 300 MHz, ^{13}C: 75 MHz), 400 (^{1}H: 400 MHz, ^{13}C: 101 MHz) or 600 (^{1}H: 600 MHz) spectrometer using perdeuterated solvents. The chemical shift δ is given in parts per million (ppm). Multiplicities were specified with the following abbreviations: s (singlet), d (doublet), t (triplet), q (quartet), quin (quintet), m (multiplet), and br (broad signal) as well as combinations thereof. ^{13}C NMR peaks were determined by DEPT 135 and DEPT 90 (distortionless enhancement by polarization transfer). NMR spectra were processed with MestReNova 11.0 (Mestrelab Research, Compostela, Spain). High-resolution mass spectrometry (HRMS) was performed on an Agilent 6540 UHD Accurate-Mass Q-TOF LC/MS system (Agilent Technologies, Santa Clara, CA) using an ESI source. Preparative HPLC was performed with a system from Waters (Milford, Massachusetts, USA) consisting of a 2524 binary gradient module, a 2489 detector, a prep injector, and a fraction collector III. A Phenomenex Gemini 5 μm NX–C18 column (110 Å, 250×21.2 mm, Phenomenex Ltd., Aschaffenburg, Germany) served as stationary phase. As mobile phase, 0.1% TFA or 0.1% NH_3 in millipore water and acetonitrile (MeCN) were used. The temperature was 25 °C, the flow rate 20 mL/min and UV detection was performed at 220 nm. Analytical HPLC experiments were performed on a 1100 HPLC system from Agilent Technologies equipped with Instant Pilot controller, a G1312 A Bin Pump, a G1329 A ALS autosampler, a G1379 A vacuum degasser, a G1316 A column compartment and a G1315B DAD detector. The column was a Phenomenex Gemini 5 μm NX–C18 column (110 Å, 250×4.6 mm, Phenomenex Ltd., Aschaffenburg, Germany) tempered at 30 °C. As mobile phase, mixtures of MeCN and aqueous TFA (for compounds **23**, **25**, **27**) or aqueous NH_3 (for compounds **24**, **26**, **28**) were used (linear gradient: MeCN/TFA (0.1%) (v/v) 0 min: 10:90, 25–35 min: 95:5, 36–45 min: 10:90; flow rate = 1.00 mL/min, t_0 = 3.21 min). Capacity factors were calculated according to $k = (t_R-t_0)/t_0$. Detection was performed at 220 nm. Furthermore, a filtration of the stock solutions with PTFE filters (25 mm, 0.2 μm, Phenomenex Ltd., Aschaffenburg, Germany) was carried out before testing. Compound purities determined by HPLC were calculated as the peak area of the analyzed compound in % relative to the total peak area (UV detection at 220 nm). The HPLC purity and stability of final compounds are displayed in the SI (cf. Figure S1–S6, SI).

Synthesis and Analytical Data

2-Bromo-1-(4-nitrophenyl)ethan-1-one (1)[65]

4-Nitroacetophenone (10.00 g, 60.54 mmol, 1 eq.) was dissolved in DCM and added to a suspension of N-bromosuccinimide (12.92 g, 72.64 mmol, 1.2 eq.) and p-toluenesulfonic acid (1.14 g, 6.06 mmol, 0.1 eq.) in DCM at room temperature. The reaction was heated to reflux overnight. The reaction was poured on water and the organic phase was separated. The aqueous phase was extracted with DCM, the combined organic phases washed with saturated bicarbonate solution and brine, dried over Na_2SO_4 and the solvent was removed under reduced pressure. The crude product was purified by column chromatography (DCM/PE 1:1). A pale yellow solid was obtained (9.41 g, 64%). $R_f = 0.61$ (PE/DCM 4:6). ^{1}H NMR (300 MHz, $CDCl_3$) δ 8.48–8.26 (m, 2H), 8.21–8.07 (m, 2H), 4.47 (s, 2H). ^{13}C NMR (75 MHz, $CDCl_3$) δ 189.92, 150.71, 138.37, 130.11, 124.08, 30.18. HRMS (EI-MS): m/z $M^{\bullet+}$ calculated for $C_8H_6NO_3Br^{\bullet+}$: 242.9526, found 242.9522; $C_8H_6NO_3Br$ (244.04).

2-Bromo-1-(4-nitrophenyl)ethan-1-ol (2)[66]

1 (3.34 g, 13.70 mmol, 1 eq.) was dissolved in MeOH. $NaBH_4$ (0.18 g, 4.80 mmol, 0.35 eq.) was added in portions at 0 °C. The reaction was stirred for 1 h at room temperature. The solvent was removed under reduced pressure and the crude product was dissolved in water. The aqueous phase was extracted with diethyl ether. The combined organic phases were washed with saturated ammonium chloride solution and brine, dried over Na_2SO_4 and the solvent was removed under reduced pressure. A slightly yellow solid was obtained (2.23 g, 66%). The product was used without further purification.

2-(4-Nitrophenyl)oxirane (3)[67]

2 (0.5 g, 2.03 mmol, 1 eq.) and K_2CO_3 (0.56 g, 4.06 mmol, 2 eq.) were dissolved in THF and heated to reflux overnight. The solid was filtered off and the solvent was removed under reduced pressure. The crude product was purified by column chromatography (PE/EtOAc 8:2). A yellow solid was obtained (0.29 g, 87%). $R_f = 0.78$ (PE/EtOAc 7:3). ^{1}H NMR (300 MHz, $CDCl_3$) δ 8.29–8.13 (m, 2H), 7.56–7.36 (m, 2H), 3.96 (dd, J = 4.1, 2.5 Hz, 1H), 3.23 (dd, J = 5.5, 4.1 Hz, 1H), 2.78 (dd, J = 5.5, 2.5 Hz, 1H). ^{13}C NMR (75 MHz, $CDCl_3$) δ 147.82, 145.26, 126.24, 123.85, 51.71, 51.48. HRMS (EI-MS): m/z $M^{\bullet+}$ calculated for $C_8H_7NO_3^{\bullet+}$: 164.0342, found 164.0339; $C_8H_7NO_3$ (165.15).

3-Chloro-4-methoxybenzaldehyde (4)[68]

Sulfurylchloride (2.41 ml, 29.38 mmol, 2 eq.) was added to a solution of 4-methoxybenzaldehyde (2.00 g, 14.69 mmol, 1 eq.) in acetic acid. The reaction was stirred overnight at room temperature and poured onto a mixture of ice and water. The white solid was filtered off, washed with ice cold water and hexanes and dried in vacuo. A white solid was obtained (2,15 g, 86%). $R_f = 0.68$ (PE/EtOAc 7:3). ^{1}H NMR (300 MHz, CDCl3) δ 9.85 (s, 1H), 7.91 (d, J = 2.0 Hz, 1H), 7.78 (dd, J = 8.5, 2.0 Hz, 1H), 7.05 (d, J = 8.5 Hz, 1H), 3.99 (s, 3H). ^{13}C NMR (75 MHz, CDCl3) δ 189.8, 159.9, 131.3, 130.6, 130.3, 123.7, 111.7, 56.5. HRMS (APCI-MS): m/z $[M+H]^+$ calculated for $C_8H_8ClO_2^+$: 171.0207, found 171.0207; $C_8H_7ClO_2$ (170.59).

ChemBioChem

Research Article
doi.org/10.1002/cbic.202300658

Chemistry Europe
European Chemical
Societies Publishing

2-Chloro-1-methoxy-4-(2-nitrovinyl)benzene (5)[69]

4 (6.40 g, 37.52 mmol, 1 eq.), nitromethane (6.03 ml, 112.56 mmol, 3 eq.) and ammonium acetate (2.40 g, 93.80 mmol, 2.5 eq.) were dissolved in acetic acid and heated to reflux for 4 h. Water was added and the reaction was extracted with DCM. The combined organic phases were washed with 1 N aq. NaOH solution and brine, dried over Na_2SO_4 and the solvent removed under reduced pressure. The crude product was purified via column chromatography (PE/EtOAc 8:2). A yellow solid was obtained (5.49 g, 68%). $R_f = 0.67$ (PE/EtOAc 7:3). ^1H NMR (300 MHz, CDCl$_3$) δ 7.90 (d, $J = 13.6$ Hz, 1H), 7.58 (d, $J = 2.2$ Hz, 1H), 7.50 (d, $J = 13.6$ Hz, 1H), 7.44 (dd, $J = 8.7$, 2.3 Hz, 1H), 6.98 (d, $J = 8.6$ Hz, 1H), 3.97 (s, 3H). ^{13}C NMR (75 MHz, CDCl$_3$) δ 158.08, 137.69, 136.02, 130.48, 129.83, 123.83, 123.33, 112.36, 56.46. HRMS (EI-MS): m/z $M^{•+}$ calculated for $C_9H_8ClNO_3^{•+}$: 213.0180, found 213.0187; $C_9H_8ClNO_3$ (213.67).

2-(3-Chloro-4-methoxyphenyl)ethan-1-amine (6)[69]

5 (5.43 g, 25.42 mmol, 1 eq.) was dissolved in THF and added slowly at room temperature to a suspension of LiAlH$_4$ (2.89 g, 76.26 mmol, 3 eq.) in THF. The reaction was heated to reflux for 3 h. After cooling to room temperature water (10 ml) and 20% aq. KOH-solution was added carefully at 0 °C and the reaction was stirred for 30 min at room temperature. The white solid was filtered off and the filtrate was dried under reduced pressure. The crude product was dried in vacuo. A yellow oil was obtained (4.44 g, 94%). $R_f = 0.05$ (DCM/MeOH 98:2). ^1H NMR (300 MHz, CDCl$_3$) δ 7.20 (d, $J = 2.1$ Hz, 1H), 7.05 (dd, $J = 8.3$, 2.2 Hz, 1H), 6.86 (d, $J = 8.4$ Hz, 1H), 3.87 (s, 3H), 2.92 (t, $J = 6.8$ Hz, 2H), 2.66 (t, $J = 6.8$ Hz, 2H), 1.49 (bs, 2H). ^{13}C NMR (75 MHz, CDCl$_3$) δ 153.45, 132.98, 130.47, 128.03, 122.26, 112.13, 56.20, 43.46, 38.78. HRMS (ESI-MS): m/z $[M+H]^+$ calculated for $C_9H_{13}ClNO^+$: 186.0680, found 186.0679; $C_9H_{12}ClNO$ (185,65).

tert-Butyl (3-Chloro-4-methoxyphenethyl)carbamate (7)

Di-tert-butyldicarbonate (3.23 g, 14.82 mmol, 1.1 eq.) was dissolved in DCM and added slowly at room temperature to a solution of **6** (2.50 g, 13.47 mmol, 1 eq.) in DCM. The reaction was stirred at room temperature overnight. The solvent was removed under reduced pressure and the crude product was dried in vacuo. A slightly yellow solid was obtained (3.79 g, 98%). $R_f = 0.48$ (PE/EtOAc 8:2). ^1H NMR (400 MHz, CDCl$_3$) δ 7.19 (d, $J = 2.1$ Hz, 1H), 7.03 (dd, $J = 8.4$, 2.1 Hz, 1H), 6.85 (d, $J = 8.4$ Hz, 1H), 3.87 (s, 3H), 3.31 (t, $J = 7.0$ Hz, 2H), 2.70 (t, $J = 7.0$ Hz, 2H), 1.42 (s, 9H). ^{13}C NMR (101 MHz, CDCl$_3$) δ 155.90, 153.61, 132.15, 130.49, 127.98, 122.33, 112.22, 56.18, 40.89, 35.11, 28.39, 23.86. HRMS (ESI-MS): m/z $[M+H]^+$ calculated for $C_{14}H_{21}ClNO_3^+$: 286.1204, found 286.1204; $C_{14}H_{20}ClNO_3$ (285.77).

2-(3-Chloro-4-methoxyphenyl)-N-methylethan-1-amine (8)[70]

7 (6.2 g, 21.70 mmol, 1 eq.) was dissolved in THF and added slowly at room temperature to a suspension of LiAlH$_4$ (2.47 g, 65.10 mmol, 3 eq.) in THF. The reaction was heated to reflux for 3 h. After cooling to room temperature water (10 ml) and 20% aq. KOH-solution was added carefully at 0 °C and the reaction was stirred for 30 min at room temperature. The white solid was filtered off and the filtrate was dried under reduced pressure. The crude product was dried in vacuo. A yellow oil was obtained (3.88 g, 90%). $R_f = 0.16$ (DCM/MeOH+1% NH$_3$ 95:5). ^1H NMR (300 MHz, CDCl$_3$) δ 7.21 (d, $J = 2.1$ Hz, 1H), 7.05 (dd, $J = 8.4$, 2.2 Hz, 1H), 6.85 (d, $J = 8.4$ Hz, 1H), 3.87 (s, $J = 3.9$ Hz, 3H), 2.84–2.76 (m, 2H), 2.76–2.68 (m, 2H), 2.43 (s, 3H). ^{13}C NMR (75 MHz, CDCl$_3$) δ 153.42, 133.24, 130.34, 127.92, 122.27, 112.13, 56.20, 53.13, 36.38, 35.03. HRMS (ESI-MS):

m/z $[M+H]^+$ calculated for $C_{10}H_{15}ClNO^+$: 200.0837, found 200.0839; $C_{10}H_{14}ClNO$ (199.69).

2-((3-Chloro-4-methoxyphenethyl)(methyl)amino)-1-(4-nitrophenyl)ethan-1-ol (9)[58]

8 (2.44 g, 12.22 mmol, 1 eq.) and **3** (2.02 g, 12.22 mmol, 1 eq.) were dissolved in acetonitrile and heated to reflux overnight. The solvent was removed under reduced pressure and the crude product was purified by column chromatography (DCM/MeOH+1% NH$_3$ 98:2). A brown oil was obtained (4.00 g, 90%). $R_f = 0.16$ (DCM/MeOH+1% NH$_3$ 98:2). ^1H NMR (300 MHz, CDCl$_3$) δ 8.23–8.12 (m, 2H), 7.57–7.47 (m, 2H), 7.20 (d, $J = 2.2$ Hz, 1H), 7.05 (dd, $J = 8.4$, 2.2 Hz, 1H), 6.86 (d, $J = 8.4$ Hz, 1H), 4.78 (dd, $J = 10.4$, 3.5 Hz, 1H), 4.19 (bs, 1H), 3.87 (s, 3H), 2.90–2.57 (m, 5H), 2.52–2.41 (m, 4H). ^{13}C NMR (75 MHz, CDCl$_3$) δ 153.54, 149.73, 147.33, 132.59, 130.34, 127.85, 126.52, 123.64, 122.32, 112.16, 68.56, 65.26, 59.18, 56.19, 41.73, 32.47. HRMS (ESI-MS): m/z $[M+H]^+$ calculated for $C_{18}H_{22}ClN_2O_4^+$: 365.1263, found 365.1268; $C_{18}H_{21}ClN_2O_4$ (364.83).

7-Chloro-8-methoxy-3-methyl-1-(4-nitrophenyl)-2,3,4,5-tetrahydro-1H-benzo[d]azepine (10)

9 (2.49 g, 7.65 mmol, 1 eq.) was dissolved in Eaton's reagent (40 ml) and stirred for 72 h at room temperature. The reaction was poured onto ice water and basified with 20% aqueous KOH-solution. The aqueous phase was extracted with DCM. The combined organic phases were washed with water, dried over Na_2SO_4 and the solvent was removed under reduced pressure. The crude product was purified by column chromatography (DCM/MeOH+1% NH$_3$ 98:2). A red solid was obtained (1.20 g, 45%). $R_f = 0.18$ (DCM/MeOH+1% NH$_3$ 98:2). ^1H NMR (300 MHz, CDCl$_3$) δ 8.22–8.10 (m, 2H), 7.37–7.28 (m, 2H), 7.14 (s, 1H), 6.39 (s, 1H), 4.42–4.27 (m, 1H), 3.71 (s, 3H), 3.26–3.13 (m, 1H), 2.96–2.75 (m, 2H), 2.73–2.52 (m, 3H), 2.38 (s, 3H). ^{13}C NMR (75 MHz, CDCl$_3$) δ 153.29, 149.94, 146.48, 141.87, 134.37, 131.64, 129.06, 123.72, 120.27, 113.44, 61.34, 57.29, 56.15, 50.27, 47.93, 34.98. HRMS (ESI-MS): m/z $[M+H]^+$ calculated for $C_{18}H_{20}ClN_2O_3^+$: 347.1157, found 347.1162; $C_{18}H_{19}ClN_2O_3$ (346.81).

8-Chloro-3-methyl-5-(4-nitrophenyl)-2,3,4,5-tetrahydro-1H-benzo[d]azepin-7-ol (11)[58]

10 (0.80 g, 2.31 mmol, 1 eq.) was dissolved DCM and cooled to −78 °C under Ar-atmosphere. BBr$_3$ (0.33 ml, 3.45 mmol, 1.5 eq.) dissolved in DCM was added at −78 °C and the reaction stirred for 1 h at this temperature and after that stirred at room temperature overnight. MeOH (5 ml) was added at −78 °C and the reaction was stirred for 1 h at room temperature. The solvent was removed under reduced pressure and the product was dried in vacuo. A brown solid was obtained (0.80 g, 84%). The product was used without further purification. HRMS (ESI-MS): m/z $[M+H]^+$ calculated for $C_{17}H_{18}ClN_2O_3^+$: 333.1000, found 333.1004; $C_{17}H_{17}ClN_2O_3$*HBr (413.70).

8-Chloro-3-methyl-5-(4-nitrophenyl)-2,3,4,5-tetrahydro-1H-benzo[d]azepin-7-yl acetate (12a)

11 (0.13 g, 0.35 mmol, 1 eq.) and NEt$_3$ (98.4 µl, 0.70 mmol, 2 eq.) were dissolved in DCM and cooled to 0 °C. Acetyl chloride (37.8 µl, 0.53 mmol, 1.5 eq.) was added slowly and the reaction was stirred at room temperature overnight. The solvent was removed under reduced pressure and the product was purified by column chromatography (98:2 DCM/MeOH). An orange solid was obtained

(0.10 g, 77%). $R_f = 0.48$ (98:2 DCM/MeOH + 1% NH$_3$). ^{1}H NMR (300 MHz, CDCl$_3$) δ 8.23–8.17 (m, 2H), 7.37–7.30 (m, 2H), 7.24 (s, 1H), 6.41 (s, 1H), 4.37 (d, $J = 7.5$ Hz, 1H), 3.09–2.91 (m, 3H), 2.81–2.73 (m, 2H), 2.54–2.45 (m, 1H), 2.40 (s, 3H), 2.27 (s, 3H). ^{13}C NMR (75 MHz, CDCl$_3$) δ 168.52, 149.57, 146.74, 145.15, 142.67, 140.44, 131.40, 129.21, 124.78, 123.98, 123.52, 61.67, 56.66, 49.53, 47.77, 35.57, 20.62. HRMS (ESI-MS): m/z [M+H]$^+$ calculated for C$_{19}$H$_{20}$ClN$_2$O$_4$$^+$: 375.1106, found 375.1113; C$_{19}$H$_{19}$ClN$_2$O$_4$ (374.82).

7-Chloro-3-methyl-1-(4-nitrophenyl)-8-((triisopropylsilyl)oxy)-2,3,4,5-tetrahydro-1H-benzo[d]azepine (12 b)

Triisopropylsilylchloride (309 μl, 1.46 mmol, 2 eq.) and imidazole (0.10 g, 1.46 mmol, 2 eq.) were dissolved in DMF. **11** (0.30 g, 0.73 mmol, 1 eq.) and NEt$_3$ (513 μl, 3.65 mmol, 5 eq.) dissolved in DMF were added at room temperature under Ar-atmosphere. The reaction was stirred overnight at room temperature and subsequently poured into water. The aqueous phase was extracted with diethyl ether. The combined organic phases were washed with saturated ammonium chloride solution and brine, dried over Na$_2$SO$_4$ and the solvent removed under reduced pressure. The crude product was purified by flash chromatography (SiO$_2$, 0 min to 20 min, 100:0 to 95:5 DCM/MeOH). $R_f = 0.40$ (DCM/MeOH 95:5). A slightly yellow solid was obtained (0.32 g, 90%). ^{1}H NMR (300 MHz, CDCl$_3$) δ 8.29–8.15 (m, 2H), 7.38–7.28 (m, 1H), 7.12 (s, 1H), 6.06 (s, 1H), 4.53–4.28 (m, 1H), 3.13–2.83 (m, 4H), 2.78–2.63 (m, 1H), 2.50–2.35 (m, 4H), 1.05–0.88 (m, 21H). ^{13}C NMR (75 MHz, CDCl$_3$) δ 150.35, 150.15, 146.69, 142.27, 134.19, 131.25, 129.22, 123.85, 122.65, 120.20, 61.91, 57.25, 49.02, 47.66, 34.92, 17.77, 12.71. HRMS (ESI-MS): m/z [M+H]$^+$ calculated for C$_{26}$H$_{38}$ClN$_2$O$_3$Si$^+$: 489.2335, found 489.2342; C$_{26}$H$_{37}$ClN$_2$O$_3$Si (488.23).

5-(4-Aminophenyl)-8-chloro-3-methyl-2,3,4,5-tetrahydro-1H-benzo[d]azepin-7-yl acetate (13 a)

12 a (0.14 g, 0.37 mmol, 1 eq.) and Pd/C (10%) (0.01 g, 10 wt%) were dissolved in a mixture of THF and MeOH (1:1) and the reaction was stirred overnight under H$_2$-atmosphere. The reaction was filtered over celite and the solvent was removed under reduced pressure. The crude product was dried *in vacuo*. A yellow solid was obtained (0.12 g, 95%). The product was used without further purification. HRMS (ESI-MS): m/z [M+H]$^+$ calculated for C$_{19}$H$_{22}$ClN$_2$O$_2$$^+$: 345.1364, found 345.1370; C$_{19}$H$_{21}$ClN$_2$O$_2$ (344.84).

4-(7-Chloro-3-methyl-8-((triisopropylsilyl)oxy)-2,3,4,5-tetrahydro-1H-benzo[d]azepin-1-yl)aniline (13 b)

12 b (0.42 g, 0.86 mmol, 1 eq.) and Pd/C (10%) (0.04 g, 10 wt%) were dissolved in a mixture of THF and MeOH (1:1) and the reaction was stirred overnight under H$_2$-atmosphere. The reaction was filtered over celite and the solvent was removed under reduced pressure. The crude product was dried *in vacuo*. A brown oil was obtained (0.38 g, 96%). The product was used without further purification. HRMS (ESI-MS): m/z [M+H]$^+$ calculated for C$_{26}$H$_{40}$ClN$_2$OSi$^+$: 459.2593, found 459.2598; C$_{26}$H$_{39}$ClN$_2$OSi (459.15).

3-(1,3-Dioxoisoindolin-2-yl)propane-1-sulfonyl chloride (14 a)[59]

Thiourea (0.38 g, 5.00 mmol, 1 eq.) and 3-bromopropylphthalimide (1.34 g, 5.00 mmol, 1 eq.) were dissolved in EtOH and heated to reflux for 1 h. The solvent was removed under reduced pressure and the resulting white solid was added to a suspension of N-chlorosuccinimide (NCS) in MeCN and 2 N aq. HCl (1.62 ml, 3.24 mmol, 0.65 eq.) at 10°C. The reaction was stirred at 10°C for 30 min and the reaction was quenched with water. The aqueous phase was extracted with diethyl ether. The organic phase was washed with brine, dried over Na$_2$SO$_4$ and the solvent was removed under reduced pressure. The crude product was purified by column chromatography (3:1 PE/EtOAc). A white solid was obtained (1.29 g, 89%). $R_f = 0.80$ (1:1 PE/EtOAc). ^{1}H NMR (300 MHz, CDCl$_3$) δ 7.90–7.82 (m, 2H), 7.79–7.72 (m, 2H), 3.89 (t, $J = 6.5$ Hz, 2H), 3.80–3.70 (m, 2H), 2.51–2.35 (m, 2H). ^{13}C NMR (75 MHz, CDCl$_3$) δ 168.20, 134.43, 131.74, 123.61, 62.86, 35.55, 24.13. HRMS (ESI-MS): m/z [M+H]$^+$ calculated for C$_{11}$H$_{11}$ClNO$_4$S$^+$: 288.0092, found 288.0092; C$_{11}$H$_{10}$ClNO$_4$S (287.71).

Ethyl 5-(chlorosulfonyl)pentanoate (14 b)[59,71]

Ethyl 5-bromovalerate (3.00 g, 14.35 mmol, 1 eq.) and thiourea (1.08 g, 14.35 mmol) were dissolved in EtOH and heated to reflux overnight. The solvent was removed under reduced pressure and the obtained solid was added at 5°C to a suspension of NCS (9.58 g, 71.75 mmol, 5 eq.) in acetonitrile and 2 N aq. HCl (5 ml). The reaction was stirred for 20 min below 10°C and poured onto water. The aqueous phase was extracted with diethyl ether. The combined organic phases were washed with brine, dried over Na$_2$SO$_4$ and the solvent was removed under reduced pressure. The crude product was purified by column chromatography (PE/EtOAc 8:2). A clear oil was obtained (2.86 g, 87%). $R_f = 0.45$ (PE/EtOAc 8:2). ^{1}H NMR (300 MHz, CDCl$_3$) δ 4.14 (q, $J = 7.1$ Hz, 2H), 3.77–3.61 (m, 2H), 2.39 (t, $J = 7.1$ Hz, 2H), 2.16–1.98 (m, 2H), 1.91–1.74 (m, 2H), 1.30–1.21 (m, 3H). ^{13}C NMR (75 MHz, CDCl$_3$) δ 172.52, 64.96, 60.72, 33.32, 23.83, 22.84, 14.23. HRMS (ESI-MS): m/z [M+H]$^+$ calculated for C$_7$H$_{14}$ClO$_4$S$^+$: 229.0296, found 229.0295; C$_7$H$_{13}$ClO$_4$S (228.69).

General procedure A

Ethylene glycol derivative (1 eq.) and NEt$_3$ (2.5 eq.) were dissolved in DCM. Methanesulfonyl chloride (2 eq.) was added at 0°C and the reaction was stirred at room temperature overnight. The white solid was filtered off and the filtrate was washed with saturated bicarbonate solution and brine, dried over Na$_2$SO$_4$ and the solvent was removed under reduced pressure. The crude product was purified by column chromatography (DCM/MeOH 98:2).

Oxybis(ethane-2,1-diyl) dimethanesulfonate (15 a)[72]

The product was synthesized following general procedure A from diethylene glycol (5.00 g, 47.12 mmol, 1 eq.), methanesulfonyl chloride (7.29 ml, 94.24 mmol, 2 eq.) and NEt$_3$ (16.42 ml, 117.80 mmol, 2.5 eq.). A yellow oil was obtained (11.87 g, 96%). $R_f = 0.80$ (DCM/MeOH 98:2). ^{1}H NMR (300 MHz, CDCl$_3$) δ 4.37–4.28 (m, 4H), 3.78–3.68 (m, 4H), 3.02 (s, 6H). ^{13}C NMR (75 MHz, CDCl$_3$) δ 69.05, 68.97, 37.57. HRMS (ESI-MS): m/z [M+H]$^+$ calculated for C$_6$H$_{15}$O$_7$S$_2$$^+$: 263.0254, found 263.0254; C$_6$H$_{14}$O$_7$S$_2$ (262.29).

(Ethane-1,2-diylbis(oxy))bis(ethane-2,1-diyl) dimethanesulfonate (15 b)[73]

The product was synthesized following general procedure A from triethylene glycol (7.00 g, 46.61 mmol, 1 eq.), methanesulfonyl chloride (7.21 ml, 93.22 mmol, 2 eq.) and NEt$_3$ (16.24 ml, 116.53 mmol, 2.5 eq.). A yellow oil was obtained (13.48 g, 94%). $R_f = 0.80$ (DCM/MeOH 98:2). ^{1}H NMR (300 MHz, CDCl$_3$) δ 4.38–4.28 (m, 4H), 3.75–3.69 (m, 4H), 3.63 (s, 4H), 3.03 (s, 6H). ^{13}C NMR (75 MHz, CDCl$_3$) δ 70.51, 69.25, 68.99, 37.62. HRMS (ESI-MS): m/z [M+H]$^+$ calculated for C$_8$H$_{19}$O$_8$S$_2$$^+$: 307.0515, found 307.0516; C$_8$H$_{18}$O$_8$S$_2$ (306.34).

ChemBioChem

Research Article
doi.org/10.1002/cbic.202300658

Chemistry Europe
European Chemical
Societies Publishing

General procedure B

The di-mesylate product (1 eq.) and sodium azide (4 eq.) were dissolved in a mixture of EtOH and DMF (4:1) and the reaction was heated to reflux overnight. The solvents were removed under reduced pressure and the crude product was dissolved in diethyl ether. The organic phase was washed with saturated ammonium chloride solution and brine, dried over Na_2SO_4 and the solvent removed under reduced pressure. The product was dried *in vacuo*.

1-Azido-2-(2-azidoethoxy)ethane (16 a)[74]

The product was synthesized following general procedure B from **15 a** (5.00 g, 19.06 mmol, 1 eq.) and sodium azide (4.96 g, 76.24 mmol, 4 eq.). A yellow oil was obtained (2.91 g, 98%). $R_f =$ 0.35 (DCM/MeOH 98:2). ^{1}H NMR (300 MHz, CDCl$_3$) δ 3.72–3.64 (m, 4H), 3.45–3.36 (m, 4H). ^{13}C NMR (75 MHz, CDCl$_3$) δ 70.10, 50.76. HRMS (APCI-MS): m/z [M+H]$^+$ calculated for $C_4H_9N_6O^+$: 157.0832, found 157.0835; $C_4H_8N_6O$ (156.15).

1,2-Bis(2-azidoethoxy)ethane (16 b)[75]

The product was synthesized following general procedure B from **15 b** (6.00 g, 19.59 mmol, 1 eq.) and sodium azide (5.09 g, 78.36 mmol, 4 eq.). A yellow oil was obtained (3.97 g, 99%). $R_f =$ 0.26 (DCM/MeOH 98:2). ^{1}H NMR (300 MHz, CDCl$_3$) δ 3.72–3.65 (m, 8H), 3.43–3.34 (m, 4H). ^{13}C NMR (75 MHz, CDCl$_3$) δ 70.76, 70.17, 50.71. HRMS (APCI-MS): m/z [M+H]$^+$ calculated for $C_6H_{13}N_6O_2^+$: 201.1095, found 201.1096; $C_6H_{12}N_6O_2$ (200.20).

General procedure C

The diazide product (1 eq.) was dissolved in a mixture of EtOAc/THF/1 N aq. HCl (5:1:5). Triphenylphosphine (1 eq.) dissolved in diethyl ether was added slowly and the reaction was stirred at room temperature overnight. The white solid was filtered off. 4 N aq. HCl was added to the filtrate and the aqueous phase was washed with diethyl ether, basified with NaOH and subsequently extracted with DCM. The organic phase was dried over Na_2SO_4 and the solvent was removed under reduced pressure. The crude product was purified by column chromatography (DCM/MeOH+ 1% NH_3 95:5).

2-(2-Azidoethoxy)ethan-1-amine (17 a)[76]

The product was synthesized following general procedure C from **16 a** (3.36 g, 21.52 mmol, 1 eq.) and triphenylphosphine (5.64 g, 21.52 mmol, 1 eq.). A clear oil was obtained (1.68 g, 60%). $R_f =$ 0.38 (DCM/MeOH+ 1% NH_3 95:5). ^{1}H NMR (300 MHz, CDCl$_3$) δ 3.88 (s, 2H), 3.64–3.59 (m, 2H), 3.58–3.52 (m, 2H), 3.39–3.31 (m, 2H), 2.92 (t, $J = 5.1$ Hz, 2H). ^{13}C NMR (75 MHz, CDCl$_3$) δ 71.47, 69.90, 50.71, 41.06. HRMS (ESI-MS): m/z [M+H]$^+$ calculated for $C_4H_{11}N_4O^+$: 131.0927, found 131.0927; $C_4H_{10}N_4O$ (130.15).

2-(2-(2-Azidoethoxy)ethoxy)ethan-1-amine (17 b)[60]

The product was synthesized following general procedure C from **16 b** (1.93 g, 9.64 mmol, 1 eq.) and triphenylphosphine (2.53 g, 9.64 mmol, 1 eq.). A clear oil was obtained (1.16 g, 69%). $R_f =$ 0.32 (DCM/MeOH+ 1% NH_3 95:5). ^{1}H NMR (300 MHz, CDCl$_3$) δ 3.70–3.57 (m, 6H), 3.53–3.46 (m, 2H), 3.41–3.33 (m, 2H), 2.91–2.78 (m, 2H), 1.55 (s, 2H). ^{13}C NMR (75 MHz, CDCl$_3$) δ 73.51, 70.68, 70.32, 70.08, 50.68, 41.77. HRMS (ESI-MS): m/z [M+H]$^+$ calculated for $C_6H_{15}N_4O_2^+$: 175.1190, found 175.1188; $C_6H_{14}N_4O_2$ (174.20).

8-Chloro-5-(4-((3-(1,3-dioxoisoindolin-2-yl)propyl)sulfonamido)phenyl)-3-methyl-2,3,4,5-tetrahydro-1H-benzo[d]azepin-7-yl acetate (18)

13 a (0.10 g, 0.29 mmol, 1 eq.) and pyridine (70 μl, 0.87 mmol, 3 eq.) were dissolved in chloroform. **14 a** (0.13 g, 0.44 mmol, 1.5 eq) was added and the reaction was stirred at 50 °C overnight. The solvent was removed under reduced pressure and the crude product was purified by column chromatography (95:5 DCM/MeOH + 1% NH_3). A yellow oil was obtained (0.11 g, 62%). $R_f = 0.30$ (95:5 DCM/MeOH + 1% NH_3). ^{1}H NMR (400 MHz, CDCl$_3$) δ 7.81–7.76 (m, 2H), 7.70–7.66 (m, 2H), 7.21–7.13 (m, 3H), 7.07–7.00 (m, 2H), 6.38 (s, 1H), 4.23 (d, $J = 8.0$ Hz, 1H), 3.84–3.72 (m, 2H), 3.26–2.68 (m, 7H), 2.48–2.33 (m, 4H), 2.29–2.13 (m, 5H). ^{13}C NMR (101 MHz, CDCl$_3$) δ 168.68, 168.26, 145.04, 144.16, 140.21, 135.37, 134.21, 131.83, 130.89, 129.52, 124.15, 123.43, 123.19, 121.27, 62.38, 56.50, 53.48, 49.17, 48.48, 47.46, 36.19, 23.24, 20.65. HRMS (ESI-MS): m/z [M+H]$^+$ calculated for $C_{30}H_{31}ClN_3O_6S^+$: 596.1617, found 596.1623; $C_{30}H_{30}ClN_3O_6S$ (596.10).

3-Amino-N-(4-(7-chloro-8-hydroxy-3-methyl-2,3,4,5-tetrahydro-1H-benzo[d]azepin-1-yl)phenyl)propane-1-sulfonamide (19)

Hydrazine hydrate (83 μl, 1.70 mmol, 10 eq.) was added to a solution of **18** (0.1 g, 0.17 mmol, 1 eq.) in EtOH and the reaction was heated to reflux overnight. The reaction was cooled to 0 °C and the white solid was filtered off. The solvent of the filtrate was evaporated under reduced pressure and the crude product was purified by preparative HPLC. A sticky solid was obtained (25 mg, 23%). ^{1}H NMR (400 MHz, MeOD) δ 7.46–7.09 (m, 5H), 6.82–5.80 (m, 1H), 4.57 (d, $J = 9.7$ Hz, 1H), 3.93–3.30 (m, 4H), 3.28–3.18 (m, 2H), 3.14–2.87 (m, 7H), 2.26–2.06 (m, 2H). HRMS (ESI-MS): m/z [M+H]$^+$ calculated for $C_{20}H_{27}ClN_3O_3S^+$: 424.1456, found 424.1459; $C_{20}H_{26}ClN_3O_3S*2$ TFA (652.00).

Ethyl 5-(N-(4-(7-chloro-3-methyl-8-((triisopropylsilyl)oxy)-2,3,4,5-tetrahydro-1H-benzo[d]azepin-1-yl)phenyl)sulfamoyl)pentanoate (20)

13 b (0.50 g, 1.01 mmol, 1 eq.) and pyridine (245 μl, 3.03 mmol, 3 eq.) were dissolved in CHCl$_3$. **14 b** (0.46 g, 2.02 mmol, 2 eq.) was added and the reaction was stirred at 50 °C overnight. DCM was added to the reaction and the organic phase was washed with water and brine, dried over Na_2SO_4 and the solvent was removed under reduced pressure. The crude product was purified by flash chromatography (SiO$_2$, 0 min to 5 min to 25 min, 98:2 to 98:2 to 9:1, DCM/MeOH). A pale yellow solid was obtained (0.37 g, 56%). $R_f = 0.20$ (DCM/MeOH 95:5). ^{1}H NMR (400 MHz, CDCl$_3$) δ 7.33–7.27 (m, 2H), 7.11–7.02 (m, 3H), 6.11 (s, 1H), 4.76–4.53 (m, 1H), 4.07 (d, $J = 7.1$ Hz, 2H), 3.63–3.30 (m, 3H), 3.16–2.95 (m, 3H), 2.86–2.73 (m, 1H), 2.73–2.52 (m, 4H), 2.34–2.23 (m, 2H), 1.91–1.62 (m, 4H), 1.20 (t, $J = 7.1$ Hz, 3H), 0.95–0.86 (m, 21H). ^{13}C NMR (101 MHz, CDCl$_3$) δ 172.99, 150.47, 142.51, 137.16, 136.69, 132.18, 130.91, 129.31, 122.63, 120.87, 120.13, 61.86, 60.50, 56.73, 51.24, 46.36, 45.59, 33.62, 23.46, 22.99, 17.76, 14.20, 12.56. HRMS (ESI-MS): m/z [M+H]$^+$ calculated for $C_{33}H_{52}ClN_2O_5SSi^+$: 651.3049, found 651.3060; $C_{33}H_{51}ClN_2O_5SSi$ (651.38).

5-(N-(4-(7-Chloro-8-hydroxy-3-methyl-2,3,4,5-tetrahydro-1H-benzo[d]azepin-1-yl)phenyl)sulfamoyl)-N-(prop-2-yn-1-yl)pentanamide (21)

20 (0.34 g, 0.52 mmol, 1 eq.) was dissolved in THF and LiOH (37 mg, 1.56 mmol, 3 eq.) dissolved in water was added and the reaction was stirred at room temperature overnight. 0.1 N HCl (32 ml,

3.12 mmol, 6 eq.) was added slowly at 0 °C. The solvents were removed by lyophilization and the residue was dissolved in DMF. HATU (236 mg, 0.62 mmol, 1.2 eq.), DIPEA (269 µl, 1.56 mmol, 6 eq.) and propargylamine (50 µl, 0.78 mmol, 1.5 eq.) were added and the reaction was stirred at room temperature overnight. The solvent was removed under reduced pressure and the crude product was purified by flash chromatography (SiO$_2$, 0 min to 5 min to 6 min to 25 min, 100:0 to 100:0 to 95:5 to 8:2, DCM/MeOH). A yellow solid was obtained (0.24 g, 92%). R$_f$ = 0.18 (DCM/MeOH 9:1). ^{1}H NMR (400 MHz, MeOD) δ 7.30–7.23 (m, 2H), 7.19–7.10 (m, 3H), 6.23 (s, 1H), 4.51 (d, J = 9.6 Hz, 1H), 3.87 (d, J = 2.5 Hz, 2H), 3.63–3.36 (m, 3H), 3.25–3.16 (m, 1H), 3.14–3.05 (m, 2H), 2.97–2.85 (m, 2H), 2.82–2.74 (m, 3H), 2.53 (t, J = 2.6 Hz, 1H), 2.24–2.13 (m, 2H), 1.83–1.71 (m, 2H), 1.71–1.57 (m, 2H). ^{13}C NMR (101 MHz, MeOD) δ 173.62, 151.81, 141.96, 137.39, 130.66, 130.42, 129.14, 120.47, 118.31, 116.68, 79.22, 70.86, 60.74, 56.28, 50.55, 45.41, 44.97, 34.63, 31.15, 28.04, 23.84, 22.80. HRMS (ESI-MS): m/z [M+H]$^+$ calculated for C$_{25}$H$_{31}$ClN$_3$O$_4$S$^+$: 504.1718, found 504.1722; C$_{25}$H$_{30}$ClN$_3$O$_4$S (504.04).

General procedure D

The alkyne (1 eq.) and the linker (1.5 eq.) were dissolved in DCM/MeOH (4:1). CuSO$_4$*5 H$_2$O (0.1 eq.) and ascorbic acid (0.3 eq.) were added and the reaction was stirred at room temperature for 72 h. The solvents were removed under reduced pressure and the crude product was purified by HPLC.

5-(N-(4-(7-Chloro-8-hydroxy-3-methyl-2,3,4,5-tetrahydro-1H-benzo[d]azepin-1-yl)phenyl)sulfamoyl)-N-((1-(2-(2-hydroxyethoxy)ethyl)-1H-1,2,3-triazol-4-yl)methyl)pentanamide (22a)

The product was synthesized following general procedure D from **21** (25 mg, 49.60 µmol, 1 eq.), **17a** (9.7 mg, 74.40 µmol, 1.5 eq.), CuSO$_4$*5 H$_2$O (1.2 mg, 4.96 µmol, 0.1 eq.) and ascorbic acid (2.62 mg, 14.88 µmol, 0.3 eq.). A white solid was obtained (7 mg, 14%). RP-HPLC: >97%, (t$_R$ = 7.34 min, k = 1.29). ^{1}H NMR (400 MHz, MeOD) δ 7.89 (s, 1H), 7.41–7.09 (m, 5H), 6.16 (s, 1H), 4.65–4.48 (m, 3H), 4.39 (s, 2H), 3.95–3.32 (m, 8H), 3.18–2.99 (m, 6H), 2.96 (s, 3H), 2.24 (t, J = 6.9 Hz, 2H), 1.87–1.61 (m, 4H). HRMS (ESI-MS): m/z [M+H]$^+$ calculated for C$_{29}$H$_{41}$ClN$_7$O$_5$S$^+$: 634.2573, found 634.2578; C$_{29}$H$_{40}$ClN$_7$O$_5$S* 3 TFA (976.26).

N-((1-(2-(2-(2-Aminoethoxy)ethoxy)ethyl)-1H-1,2,3-triazol-4-yl)methyl)-5-(N-(4-(7-chloro-8-hydroxy-3-methyl-2,3,4,5-tetrahydro-1H-benzo[d]azepin-1-yl)phenyl)sulfamoyl)pentanamide (22b)

The product was synthesized following general procedure D from **21** (25 mg, 49.60 µmol, 1 eq.), **17b** (13 mg, 74.40 µmol, 1.5 eq.), CuSO$_4$*5 H$_2$O (1.2 mg, 4.96 µmol, 0.1 eq.) and ascorbic acid (2.62 mg, 14.88 µmol, 0.3 eq.). A white solid was obtained (4 mg, 8%). RP-HPLC: >97%, (t$_R$ = 7.50 min, k = 1.34). ^{1}H NMR (400 MHz, MeOD) δ 7.87 (s, 1H), 7.42–7.08 (m, 5H), 6.16 (s, 1H), 4.63–4.46 (m, 3H), 4.40 (s, 2H), 3.95–3.44 (m, 12H), 3.19–2.98 (m, 6H), 2.96 (s, 3H), 2.24 (t, J = 6.9 Hz, 2H), 1.85–1.66 (m, 4H). HRMS (ESI-MS): m/z [M+H]$^+$ calculated for C$_{31}$H$_{45}$ClN$_7$O$_6$S$^+$: 678.2835, found 678.2841; C$_{31}$H$_{43}$ClN$_6$O$_7$S* 3 TFA (1020.32).

General procedure E

The primary amine (1.5 eq.) was dissolved in DMF (30 µL). NEt$_3$ (10 eq.) and the fluorescent dye NHS-ester (1 eq.) in DMF (60 µL) were added, and the reaction was shaken for 2.5 h in the dark at room temperature. The reaction was quenched with 10% aqueous TFA (20 µL), and the crude product was purified by preparative HPLC.

5-((3-(N-(4-(7-Chloro-8-hydroxy-3-methyl-2,3,4,5-tetrahydro-1H-benzo[d]azepin-1-yl)phenyl)sulfamoyl)propyl)carbamoyl)-2-(6-(dimethylamino)-3-(dimethyliminio)-3H-xanthen-9-yl)benzoate (23)

The product was synthesized following general procedure E from **19** (1.86 mg, 2.85 µmol, 1.5 eq), NEt$_3$ (2.53 µl, 19 µmol, 10 eq.) and 5-carboxytetramethylrhodamine succinimidyl ester (5-TAMRA NHS ester) (1.00 mg, 1.90 µmol, 1 eq.). A pink solid was obtained (1.6 mg, 89%). RP-HPLC: >97%, (t$_R$ = 11.27 min, k = 2.51). HRMS (ESI-MS): m/z [M+H]$^+$ calculated for C$_{45}$H$_{47}$ClN$_5$O$_7$S$^+$: 836.2879, found 836.2884; C$_{45}$H$_{46}$ClN$_5$O$_7$S* TFA (950.28).

(E)-1-(6-((3-(N-(4-(7-Chloro-8-hydroxy-3-methyl-2,3,4,5-tetrahydro-1H-benzo[d]azepin-1-yl)phenyl)sulfamoyl)propyl)amino)-6-oxohexyl)-2-((E)-3-(1-(2-methoxyethyl)-3-methyl-5-sulfo-3-(3-sulfopropyl)-3H-indol-1-ium-2-yl)allylidene)-3-methyl-3-(3-sulfopropyl)indoline-5-sulfonate (24)

The product was synthesized following general procedure E from **19** (0.25 mg, 0.38 µmol, 2 eq.) NEt$_3$ (0.25 µl, 1.90 µmol, 10 eq.), DY-549P1-NHS-ester (0.2 mg, 0.19 µmol, 1 eq.). A pink solid was obtained (0.1 mg, 39%). RP-HPLC: >97%, (t$_R$ 3.59 min, k = 0.21). HRMS (ESI-MS): m/z [M-2H]$^{2-}$ calculated for C$_{56}$H$_{70}$ClN$_5$O$_{17}$S^{2-}: 639.6535, found 639.6545; C$_{56}$H$_{72}$ClN$_5$O$_{17}$S*3 NH$_3$ (1335.06).

2-(3,6-Bis(dimethylamino)xanthylium-9-yl)-5-((2-(2-(4-((5-(N-(4-(7-chloro-8-hydroxy-3-methyl-2,3,4,5-tetrahydro-1H-benzo[d]azepin-1-yl)phenyl)sulfamoyl)pentanamido)methyl)-1H-1,2,3-triazol-1-yl)ethoxy)ethyl)carbamoyl)benzoate (25)

The product was synthesized following general procedure E from **22a** (3.16 mg, 3.24 µmol, 1.5 eq), NEt$_3$ (3.04 µl, 21.60 µmol, 10 eq.) and 5-carboxytetramethylrhodamine succinimidyl ester (5-TAMRA NHS ester) (1.14 mg, 2.16 µmol, 1 eq.). A pink solid was obtained (1.4 mg, 51%). RP-HPLC: >98%, (t$_R$ = 10.69 min, k = 2.33). HRMS (ESI-MS): m/z [M+H]$^+$ calculated for C$_{54}$H$_{61}$ClN$_9$O$_9$S$^+$: 1046.3996, found 1046.3995; C$_{54}$H$_{60}$ClN$_9$O$_9$S*2 TFA (1274.68).

2-((E)-3-((E)-1-(6-((2-(2-(4-((5-(N-(4-(7-Chloro-8-hydroxy-3-methyl-2,3,4,5-tetrahydro-1H-benzo[d]azepin-1-yl)phenyl)sulfamoyl)pentanamido)methyl)-1H-1,2,3-triazol-1-yl)ethoxy)ethyl)amino)-6-oxohexyl)-3-methyl-5-sulfonato-3-(3-sulfonatopropyl)indolin-2-ylidene)prop-1-en-1-yl)-1-(2-methoxyethyl)-3-methyl-3-(3-sulfonatopropyl)-3H-indol-1-ium-5-sulfonate (26)

The product was synthesized following general procedure E from **22a** (0.28 mg, 0.29 µmol, 1.5 eq.), NEt$_3$ (0.27 µl, 1.90 µmol, 10 eq.), DY-549P1-NHS-ester (0.2 mg, 0.19 µmol, 1 eq.). A pink solid was obtained (0.14 mg, 47%). RP-HPLC: >96%, (t$_R$ = 3.60 min, k = 0.12). HRMS (ESI-MS): m/z [M-2H]$^{2-}$ calculated for C$_{65}$H$_{84}$ClN$_9$O$_{19}$S$_5$$^{2-}$: 744.7093, found 744.7106; C$_{65}$H$_{86}$ClN$_9$O$_{19}$S$_5$*3 NH$_3$ (1544.29).

ChemBioChem

Research Article
doi.org/10.1002/cbic.202300658

Chemistry Europe
European Chemical
Societies Publishing

2-(3,6-Bis(dimethylamino)xanthylium-9-yl)-5-((2-(2-(2-(4-((5-(N-(4-(7-chloro-8-hydroxy-3-methyl-2,3,4,5-tetrahydro-1H-benzo[d]azepin-1-yl)phenyl)sulfamoyl)pentanamido)methyl)-1H-1,2,3-triazol-1-yl)ethoxy)ethoxy)ethyl)carbamoyl)benzoate (27)

The product was synthesized following general procedure E from **22 b** (2.64 mg, 2.59 μmol, 1.5 eq), NEt$_3$ (2.43 μl, 17.30 μmol, 10 eq.) and 5-carboxytetramethylrhodamine succinimidyl ester (5-TAMRA NHS ester) (0.91 mg, 1.73 μmol, 1 eq.). A pink solid was obtained (1.71 mg, 75%). RP-HPLC: >95%, (t$_R$ = 10.75 min, k = 2.35). HRMS (ESI-MS): m/z [M+H]$^+$ calculated for C$_{56}$H$_{65}$ClN$_9$O$_{10}$S$^+$: 1090.4258, found 1090.4258; C$_{56}$H$_{64}$ClN$_9$O$_{10}$S*2 TFA (1318.74).

2-((E)-3-((E)-1-(6-((2-(2-(2-(4-((5-(N-(4-(7-Chloro-8-hydroxy-3-methyl-2,3,4,5-tetrahydro-1H-benzo[d]azepin-1-yl)phenyl)sulfamoyl)pentanamido)methyl)-1H-1,2,3-triazol-1-yl)ethoxy)ethoxy)ethyl)amino)-6-oxohexyl)-3-methyl-5-sulfonato-3-(3-sulfonatopropyl)indolin-2-ylidene)prop-1-en-1-yl)-1-(2-methoxyethyl)-3-methyl-3-(3-sulfonatopropyl)-3H-indol-1-ium-5-sulfonate (28)

The product was synthesized following general procedure E from **22 b** (0.30 mg, 0.29 μmol, 1.5 eq.), NEt$_3$ (0.27 μl, 1.90 μmol, 10 eq.), DY-549P1-NHS-ester (0.2 mg, 0.19 μmol, 1 eq.). A pink solid was obtained (0.14 mg, 47%). RP-HPLC: >95%, (t$_R$ = 3.78 min, k = 0.18). HRMS (ESI-MS): m/z [M+2H]$^{2+}$ calculated for C$_{67}$H$_{92}$ClN$_9$O$_{20}$S$_5$$^{2+}$: 768.7370, found 768.7386; C$_{67}$H$_{90}$ClN$_9$O$_{20}$S$_5$*3 NH$_3$ (1588.34).

Radioligand competition binding experiments at the dopamine receptors

Cell homogenates containing the D$_{2long}$R, D$_3$R, and D$_{4.4}$R were kindly provided by Dr. Lisa Forster, University of Regensburg. Homogenates containing the D$_1$R and D$_5$R were prepared and radioligand binding experiments with cell homogenates were performed as previously described with minor modifications.[77,78] For radioligand competition binding assays homogenates were incubated in BB at a final concentration of 0.3 μg (D$_1$R), 0.3 μg (D$_{2long}$R), 0.7 μg (D$_3$R), 0.5-1.0 μg (D$_{4.4}$R), or 0.4 μg (D$_5$R) protein/well. [^{3}H]SCH-23390 (D$_1$R (K$_d$ = 0.40 nM) and D$_5$R (K$_d$ = 0.40 nM)) was added in final concentrations of 1.0 nM (D$_1$R) and 1.0 nM (D$_5$R). [^{3}H]N-methylspiperone (D$_{2long}$R (K$_d$ = 0.015 nM), D$_3$R (K$_d$ = 0.026 nM), D$_{4.4}$R (K$_d$ = 0.078 nM)) was added in final concentrations of 0.05 nM (D$_{2long}$R, D$_3$R) or 0.1 nM (D$_{4.4}$R). Non labelled compounds were added in increasing concentrations for the displacement of the radioligands. After incubation of 60 min (D$_{2long}$R, D$_3$R, and D$_{4.4}$R) or 120 min (D$_1$R and D$_5$R) at room temperature, bound radioligand was separated from free radioligand through PEI-coated GF/C filters using a Brandel harvester (Brandel Inc., Unterföhring, Germany), filters were transferred to (flexible) 1450–401 96-well sample plates (PerkinElmer, Rodgau, Germany) and after incubation with scintillation cocktail (Rotiszint eco plus, Carl Roth, Karlsruhe, Germany) for at least 3 h, radioactivity was measured using a MicroBeta2 plate counter (PerkinElmer, Waltham, MA, USA). Competition binding curves were fitted using a four-parameter fit ("log(agonist) vs. response-variable slope"). Calculations of pKi values with SEM and graphical presentations were conducted with GraphPad Prism 9 software (San Diego, CA, USA).

G$_s$ heterotrimer dissociation assay

HEK293 A cells (Thermo Fisher) were transiently transfected with the G$_s$ BRET sensor, G$_s$-CASE (http://www.addgene.org/168124/),[62] along with either D$_1$R or D$_5$R using polyethyleneimine (PEI). Per well

of a 96-well plate, 100 μl of freshly resuspended cells were incubated with 100 ng total DNA mixed with 0.3 μl PEI solution (1 mg/ml) in 10 μl Opti-MEM (Thermo Fisher), seeded onto poly-D-lysine (PDL)-pre-coated white, F-bottom 96-well plates (Brand GmbH) and cultivated at 37°C, 5% CO$_2$ in penicillin (100 U/ml)/streptomycin (0.1 mg/ml)-, 2 mM L-glutamin- and 10% fetal calf serum (FCS)-supplemented Dulbecco's modified Eagle's medium (DMEM; Thermo Fisher). 48 hours after transfection, cells were washed with Hank's Buffered Salt Solution (HBSS) and incubated with a 1/1000 furimazine (Promega) dilution in HBSS for 2 minutes. Next, the baseline BRET ratio was recorded in three consecutive reads, cells were stimulated with serial dilutions of **25** or vehicle control, and BRET was recorded for another 15 reads. For experiments in antagonist mode, serial dilutions of **25** were added together with furimazine before the experiment and 1 μM dopamine or vehicle control was added after the first three baseline recordings. All experiments were conducted using a ClarioStar Plus Plate reader (BMG Labtech) with a cycle time of 120 seconds, 0.3 seconds integration time and a focal height of 10 mm. Monochromators were used to collect the NanoLuc emission intensity between 430 and 510 nm and cpVenus emission between 500 and 560 nm. BRET ratios were defined as acceptor emission/donor emission. The basal BRET ratio before ligand stimulation (Ratio$_{basal}$) was defined as the average of all three baselaine BRET values. Ligand-induced ΔBRET was calculated for each well as a percent over basal ([(Ratio$_{stim}$ − Ratio$_{basal}$)/Ratio$_{basal}$]×100). To correct for non-pharmacological effects, the average ΔBRET of vehicle control was subtracted.

Fluorescence properties

Excitation and emission spectra of **25–28** were recorded in PBS (137 mM NaCl, 2.7 mM KCl, 10 mM Na$_2$HPO$_4$, 1.8 mM KH$_2$PO$_4$, pH 7.4) containing 1% BSA (Sigma-Aldrich, Munich, Germany) using a Cary Eclipse spectrofluorometer (Varian Inc., Mulgrave, Victoria, Australia) at 22°C, using acryl cuvettes (10×10 mm, Sarstedt, Nümbrecht, Germany). The slit adjustments (excitation/emission) were 5/10 nm for excitation spectra and 10/5 nm for emission spectra. Net spectra were calculated by subtracting the respective vehicle reference spectrum, and corrected emission spectra were calculated by multiplying the net emission spectra with the respective lamp correction spectrum. The quantum yield of **25–28** was determined according to previously described procedures[63,79] with minor modifications using a Cary Eclipse spectrofluorometer (Varian Inc., Mulgrave, Victoria, Australia) at 22°C, using acryl cuvettes (10×10 mm, Sarstedt, Nümbrecht, Germany) and cresyl violet perchlorate (Biomol GmbH–Life Science Shop, Hamburg, Germany) as a red fluorescent standard. Absorption spectra were recorded with UV/Vis spectroscopy (350-850 nm, scan rate: 300 nm/min, slits: fixed 2 nm) at a concentration of 2 μM for cresyl violet (in EtOH, λ$_{abs,max}$ = 575 nm) and **25–28** (in PBS buffer and PBS + 1% BSA, λ$_{abs,max}$ = 559–561 nm). The excitation wavelength for the emission spectra was 527 nm (**16**) or 555 nm (**17, 20**). The emission wavelength collected during the excitation scan was 630 nm. The quantum yields were calculated for three different slit adjustments (exc./em.): 5/5 nm, 10/5 nm, 10/10 nm. The means of the quantum yields, absorption, and emission maxima are presented in Table 3.

Live cell confocal microscopy at the D$_1$R

Confocal images were recorded with kind assistance from Manel Bosch (Universitat de Barcelona). HEK293T cells were transfected based on previously described procedures with the D$_1$R-YFP (C-terminally tagged) with minor modifications.[80,81,22] Cells were seeded in 35 mm wells containing 1.5 cover slips. 48 h after

transfection medium was changed to OptiMem media (Gibco) supplemented with 10 mM HEPES. Imaging was performed using a Zeiss LSM880 Laser Scanning Confocal Microscope equipped with a "Plan-Apochromat" 40x/1,3 Oil DIC M27 objective and a photo-multiplier tube (PTM) detector. For excitation of **25** an DPSS laser with a wavelength of 561 nm was used. Fluorescence was detected within an emission window of 569–669 nm. Image size was set to 512×512 pixels. After adjusting the focus, time-lapse images were recorded in intervals between 0.32 and 1 s. **25** was added in a final concentration of 50 nM. Dissociation was induced by the addition of SCH-23390 (50 μM, 1,000-fold excess). Time-lapse confocal images were processed using the ImageJ software. Contrast was adjusted for each file to facilitate the visualization of the fluorescence signal. Total fluorescence was plotted as a function of time using GraphPad Prism9 software (GraphPad, San Diego, USA). The time of addition of **25** was set as 0 min. Data was fitted using the "Association–one conc. of hot ligand" or "association then dissociation" functions from Prism9. Kon, Koff, and kinetic Kd values were calculated by Prism9.

Molecular Brightness

HEK-293AD cells were seeded in 8-well Ibidi μ-slides with a density of 25,000 cells per well and transfected with 2 μg hD$_1$R-mNeon-Green after 24 h using JetPrime transfection reagent according to manufacturer's protocol. After further 24 h cells were washed and imaged in FRET-buffer (144 mM NaCl, 5.4 mM KCl, 1 mM MgCl$_2$, 2 mM CaCl$_2$, 10 mM HEPES) on a confocal laser scanning micro-scope, Leica SP8, with a white-light laser at wavelengths of 488 and 552 nm, and laser power of 5%. All measurements were conducted with an HC PLAP CS2 40×1.3 numerical aperture (NA) oil immersion objective (Leica). Movies were acquired at 1.3 seconds per frame for 100 frames with two hybrid detectors in the range of 498 to 547 nm and 562 to 612 nm respectively, in a line sequential, counting mode. Molecular brightness ε and number of molecules N are calculated from the average (k) of the photon counts collected in a pixel and its variance (σ) according to the formulas $\varepsilon = \sigma^2/k - 1$ and $N = k^2/\sigma^2$. ImageJ was used to extract molecular brightness and fluorescence intensity values, number of emitters was calculated with Word Excel and obtained values were plotted and fitted with Prism v. 9.5.1.

Notes

The authors declare no competing financial interest.

Supporting Information

The Supporting Information is available free of charge at link DOI: XXX/number

Chemical purity and stability (Figure S1-S6), Dopamine-induced G$_s$ activation (Figure S7), Confocal microscopy (Figure S8), NMR spectra (Figure S9–S25), Structures of the fluorescent ligands **23**–**28** (Figure S26-S31), Binding poses of SKF-83959 bound to the D$_1$R (Figure S32) (PDF).

Author Contributions

The authors contributed as follows: N.R.: synthesis and analytics of the compounds, radioligand binding studies, fluorescence properties, cell culture for confocal microscopy, confocal micro-scopy, and manuscript writing. D.M.: radioligand binding studies, preparation of mNeonGreen constructs. M.N.: synthesis and radioligand binding studies. H.S.: G$_s$ heterotrimer dissocia-tion assay, manuscript writing. A.S.: Molecular Brightness studies, manuscript writing. N.K.: Molecular Brightness studies. I.R.-R.: Cell culture for confocal microscopy, supervision. G.N.: Cell culture for confocal microscopy, conception, supervision. R.F.: conception, providing infrastructure. P.K.: conception, providing infrastructure. P.A.: conception, manuscript writing, providing infrastructure. S.P.: conception, project administra-tion, manuscript writing, confocal microscopy, providing infra-structure. The data were analyzed and discussed by all authors. All authors have approved the final version of the manuscript.

Conflict of Interests

The authors declare no conflict of interest.

Data Availability Statement

The data that support the findings of this study are available from the corresponding author upon reasonable request.

[1] J.-M. Beaulieu, R. R. Gainetdinov, *Pharmacol. Rev.* **2011**, *63*, 182–217.
[2] A. Darhstrom, *Acta Physiol. Scand.* **1964**, *62*, 5–55.

[3] N.-E. Andén, A. Carlsson, A. Dahlström, K. Fuxe, N.-Å. Hillarp, K. Larsson, *Life Sci.* **1964**, *3*, 523–530.

[4] C. Missale, S. R. Nash, S. W. Robinson, M. Jaber, M. G. Caron, *Physiol. Rev.* **1998**, *78*, 189–225.

[5] J.-M. Beaulieu, S. Espinoza, R. R. Gainetdinov, *Br. J. Pharmacol.* **2015**, *172*, 1–23.

[6] J. W. Kebabian, *Life Sci.* **1978**, *23*, 479–483.

[7] P. Spano, S. Govoni, M. Trabucchi, *Adv. Biochem. Psychopharmacol.* **1978**, *19*, 155–165.

[8] A. Carlsson, *Science* **2001**, *294*, 1021–1024.

[9] O. Civelli, J. R. Bunzow, D. K. Grandy, *Annu. Rev. Pharmacol. Toxicol.* **1993**, *33*, 281–307.

[10] P. Seeman, J. Schwarz, J.-F. Chen, H. Szechtman, M. Perreault, G. S. McKnight, J. C. Roder, R. Quirion, P. Boksa, L. K. Srivastava, K. Yanai, D. Weinshenker, T. Sumiyoshi, *Synapse* **2006**, *60*, 319–346.

[11] D. R. Sibley, F. J. J. Monsma, *Trends Pharmacol. Sci.* **1992**, *13*, 61–69.

[12] P. Sokoloff, M. Andrieux, R. Besançon, C. Pilon, M.-P. Martres, B. Giros, J.-C. Schwartz, *Eur. J. Pharmacol.* **1992**, *225*, 331–337.

[13] D. Vallone, R. Picetti, E. Borrelli, *Neurosci. Biobehav. Rev.* **2000**, *24*, 125–132.

[14] L. Donnelly, J. Rathbone, C. E. Adams, *Cochrane Database Syst Rev* **2013**, *8*, CD001951.

[15] K. M. Shannon, J. P. J. Bennett, J. H. Friedman, *Neurology* **1997**, *49*, 724–728.

[16] R. Albibi, R. W. McCallum, *Ann. Intern. Med.* **1983**, *98*, 86–95.

[17] A. Grenader, D. P. Healy, *J. Pharmacol. Exp. Ther.* **1991**, *258*, 193–198.

[18] W. C. J. Oliver, G. A. Nuttall, K. J. Cherry, P. A. Decker, T. Bower, M. H. Ereth, *Anesth. Analg.* **2006**, *103*, 833–840.

[19] D. M. Mottola, W. K. Brewster, L. L. Cook, D. E. Nichols, R. B. Mailman, *J. Pharmacol. Exp. Ther.* **1992**, *262*, 383–393.

[20] P. J. Blanchet, J. Fang, M. Gillespie, L. Sabounjian, K. W. Locke, R. Gammans, M. M. Mouradian, T. N. Chase, *Clin. Neuropharmacol.* **1998**, *21*, 339–343.

[21] A. Nishi, M. Kuroiwa, T. Shuto, *Front Neuroanat* **2011**, *5*, 43.

[22] M. Rodríguez-Ruiz, E. Moreno, D. Moreno-Delgado, G. Navarro, J. Mallol, A. Cortés, C. Lluís, E. I. Canela, V. Casadó, P. J. McCormick, R. Franco, *Mol. Neurobiol.* **2017**, *54*, 4537–4550.

[23] M. Dziedzicka-Wasylewska, A. Faron-Górecka, J. Andrecka, A. Polit, M. Kuśmider, Z. Wasylewski, *Biochemistry* **2006**, *45*, 8751–8759.

[24] D. Marcellino, S. Ferré, V. Casadó, A. Cortés, B. Le Foll, C. Mazzola, F. Drago, O. Saur, H. Stark, A. Soriano, C. Barnes, S. R. Goldberg, C. Lluis, K. Fuxe, R. Franco, *J. Biol. Chem.* **2008**, *283*, 26016–26025.

[25] J. C. McGrath, S. Arribas, C. J. Daly, *Trends Pharmacol. Sci.* **1996**, *17*, 393–399.

[26] J. Mellentin-Michelotti, L. T. Evangelista, E. E. Swartzman, S. J. Miraglia, W. E. Werner, P. M. Yuan, *Anal. Biochem.* **1999**, *272*, 182–190.

[27] M. Soave, S. J. Briddon, S. J. Hill, L. A. Stoddart, *Br. J. Pharmacol.* **2020**, *177*, 978–991.

[28] L. A. Stoddart, C. W. White, K. Nguyen, S. J. Hill, K. D. G. Pfleger, *Br. J. Pharmacol.* **2016**, *173*, 3028–3037.

[29] N. C. Dale, E. K. M. Johnstone, C. W. White, K. D. G. Pfleger, *Front Bioeng Biotechnol* **2019**, *7*, 56.

[30] A. Emami-Nemini, T. Roux, M. Leblay, E. Bourrier, L. Lamarque, E. Trinquet, M. J. Lohse, *Nat. Protoc.* **2013**, *8*, 1307–1320.

[31] D. Axelrod, *J. Cell Biol.* **1981**, *89*, 141–145.

[32] S. Pockes, K. Tropmann, *Future Med. Chem.* **2021**, *13*, 1073–1081.

[33] L. Grätz, K. Tropmann, M. Bresinsky, C. Müller, G. Bernhardt, S. Pockes, *Sci. Rep.* **2020**, *10*, 13288.

[34] N. Rosier, L. Grätz, H. Schihada, J. Möller, A. Işbilir, L. J. Humphrys, M. Nagl, U. Seibel, M. J. Lohse, S. Pockes, *J. Med. Chem.* **2021**, *64*, 11695–11708.

[35] L. Forster, S. Pockes, *Sci. Rep.* **2022**, *12*, 9637.

[36] D. Capelli, C. Parravicini, G. Pochetti, R. Montanari, C. Temporini, M. Rabuffetti, M. L. Trincavelli, S. Daniele, M. Fumagalli, S. Saporiti, E. Bonfanti, M. P. Abbracchio, I. Eberini, S. Ceruti, E. Calleri, E. Capaldi, *Front. Chem.* **2019**, *7*, 910.

[37] S. Krämer, A. Moritz, L. Stehl, M. Hutt, M. Hofmann, C. Wagner, S. Bunk, D. Maurer, G. Roth, J. Wöhrle, *Sci. Rep.* **2023**, *13*, 5290.

[38] E. A. Widder, *Science* **2010**, *328*, 704–708.

[39] A. Allikalt, S. Kopanchuk, A. Rinken, *Eur. J. Pharmacol.* **2018**, *839*, 40–46.

[40] V. Bakthavachalam, N. Baindur, B. K. Madras, J. L. Neumeyer, *J. Med. Chem.* **1991**, *34*, 3235–3241.

[41] F. J. J. Monsma, A. C. Barton, H. C. Kang, D. L. Brassard, R. P. Haugland, D. R. Sibley, *J. Neurochem.* **1989**, *52*, 1641–1644.

[42] C. Iliopoulos-Tsoutsouvas, R. N. Kulkarni, A. Makriyannis, S. P. Nikas, *Expert Opin. Drug Discovery* **2018**, *13*, 933–947.

[43] A. Drakopoulos, M. Decker, *ChemPlusChem* **2020**, *85*, 1354–1364.

[44] F. Ciruela, K. A. Jacobson, V. Fernández-Dueñas, *ACS Chem. Biol.* **2014**, *9*, 1918–1928.

[45] J. A. Bourne, *CNS Drug Rev.* **2001**, *7*, 399–414.

[46] D. A. Burnett, W. J. Greenlee, B. Mckirtrick, J. Su, Z. Zhu, T. K. Sasikumar, R. Mazzola, L. Qiang, Y. Ye, *New Indane-Fused 2,3,4,5-Tetrahydro-1H-Benzo(d)Azepine Derivatives Useful for Treating Metabolic Disorder, Eating Disorder, Diabetes, Obsessive-Compulsive Disorder and Autism* **2005**, US 2005075325.

[47] J. Zhang, B. Xiong, X. Zhen, A. Zhang, *Med. Res. Rev.* **2009**, *29*, 272–294.

[48] P. Xiao, W. Yan, L. Gou, Y.-N. Zhong, L. Kong, C. Wu, X. Wen, Y. Yuan, S. Cao, C. Qu, X. Yang, C.-C. Yang, A. Xia, Z. Hu, Q. Zhang, Y.-H. He, D.-L. Zhang, C. Zhang, G.-H. Hou, H. Liu, L. Zhu, P. Fu, S. Yang, D. M. Rosenbaum, J.-P. Sun, Y. Du, L. Zhang, X. Yu, Z. Shao, *Cell* **2021**, *184*, 943–956.e18.

[49] Y. Zhuang, P. Xu, C. Mao, L. Wang, B. Krumm, X. E. Zhou, S. Huang, H. Liu, X. Cheng, X.-P. Huang, D.-D. Shen, T. Xu, Y.-F. Liu, Y. Wang, J. Guo, Y. Jiang, H. Jiang, K. Melcher, B. L. Roth, Y. Zhang, C. Zhang, H. E. Xu, *Cell* **2021**, *184*, 931–942.e18.

[50] T. Kshirsagar, A. H. Nakano, P.-Y. Law, R. Elde, P. S. Portoghese, *Neurosci. Lett.* **1998**, *249*, 83–86.

[51] R. Huisgen, *Angew. Chem. Int. Ed. Engl.* **1963**, *2*, 565–598.

[52] H. C. Kolb, M. G. Finn, K. B. Sharpless, *Angew. Chem. Int. Ed. Engl.* **2001**, *40*, 2004–2021.

[53] R. Berg, B. F. Straub, *Beilstein J. Org. Chem.* **2013**, *9*, 2715–2750.

[54] T. Laasfeld, R. Ehrminger, M.-J. Tahk, S. Veiksina, K. R. Kõlvart, M. Min, S. Kopanchuk, A. Rinken, *Nanoscale* **2021**, *13*, 2436–2447.

[55] S. Rüttinger, B. Lamarre, A. E. Knight, *Journal Fluoresc* **2008**, *18*, 1021–1026.

[56] B. Qiu, M. C. Simon, *Bio Protoc* **2016**, *6*, e1912.

[57] J. L. Neumeyer, N. Baindur, H. B. Niznik, H. C. Guan, P. Seeman, *J. Med. Chem.* **1991**, *34*, 3366–3371.

[58] J. Shen, L. Zhang, W. Song, T. Meng, X. Wang, L. Chen, L. Feng, Y. Xu, J. Shen, *Acta Pharmacol Sin* **2013**, *34*, 441–452.

[59] Z. Yang, J. Xu, *Synthesis* **2013**, *45*, 1675–1682.

[60] S. S. Iyer, A. S. Anderson, S. Reed, B. Swanson, J. G. Schmidt, *Tetrahedron Lett.* **2004**, *45*, 4285–4288.

[61] M. Bresinsky, A. Shahraki, P. Kolb, S. Pockes, H. Schihada, *J. Med. Chem.* **2023**, *66*, 15025–15041.

[62] H. Schihada, R. Shekhani, G. Schulte, *Sci. Signaling* **2021**, *14*, eabf1653.

[63] M. Keller, D. Erdmann, N. Pop, N. Pluym, S. Teng, G. Bernhardt, A. Buschauer, *Bioorg. Med. Chem.* **2011**, *19*, 2859–2878.

[64] A. Işbilir, R. Serfling, J. Möller, R. Thomas, C. De Faveri, U. Zabel, M. Scarselli, A. G. Beck-Sickinger, A. Bock, I. Coin, M. J. Lohse, P. Annibale, *Nat. Protoc.* **2021**, *16*, 1419–1451.

[65] W. Borzęcka, I. Lavandera, V. Gotor, *J. Org. Chem.* **2013**, *78*, 7312–7317.

[66] W. Wierenga, A. W. Harrison, B. R. Evans, C. G. Chidester, *J. Org. Chem.* **1984**, *49*, 438–442.

[67] C. O. Guss, H. G. Mautner, *J. Org. Chem.* **1951**, *16*, 887–891.

[68] J. Sterling, Y. Herzig, T. Goren, N. Finkelstein, D. Lerner, W. Goldenberg, I. Miskolczi, S. Molnar, F. Rantal, T. Tamas, G. Toth, A. Zagyva, A. Zekany, J. Finberg, G. Lavian, A. Gross, R. Friedman, M. Razin, W. Huang, B. Krais, M. Chorev, M. B. Youdim, M. Weinstock, *J. Med. Chem.* **2002**, *45*, 5260–5279.

[69] L. Moreno, J. Párraga, A. Galán, N. Cabedo, J. Primo, D. Cortes, *Bioorg. Med. Chem.* **2012**, *20*, 6589–6597.

[70] J. F. Bower, P. Szeto, T. Gallagher, *Org. Biomol. Chem.* **2007**, *5*, 143–150.

[71] C. J. Watkins, M. M. R. Romero, K. G. Moore, J. Ritchie, P. W. Finn, I. Kalvinsh, E. Loza, K. Dikovska, V. Gailite, M. Vorona, I. Piskunova, I. Starchenkov, V. Adrianov, C. J. Harris, J. E. S. Duffy, *Carbamic Acid Compounds Comprising a Sulfonamide Linkage as Hdac Inhibitors*, **2001**, WO0230879 A2.

[72] S. Bai, S. Li, J. Xu, X. Peng, K. Sai, W. Chu, Z. Tu, C. Zeng, R. H. Mach, *J. Med. Chem.* **2014**, *57*, 4239–4251.

[73] M. Andrus, T. Turner, J. Prince, *Multiple Drug Resistance Reversal Agent*, **2001**, WO2001060387 A1.

[74] J. M. Lehn, W. G. Skene, *Dynamers: Polymeric Materials Exhibiting Reversible Formation and Component Exchange* **2003**, WO2004003044 A2.

[75] O. A. Gansow, A. R. Kausar, K. B. Triplett, *J. Heterocycl. Chem.* **1981**, *18*, 297–302.

[76] L. T. M. Van Wandelen, J. Van Ameijde, A. S. A. Mady, A. E. M. Wammes, A. Bode, A. J. Poot, R. Ruijtenbeek, R. M. J. Liskamp, *ChemMedChem* **2012**, *7*, 2113–2121.

[77] L. Forster, L. Grätz, D. Mönnich, G. Bernhardt, S. Pockes, *Int. J. Mol. Sci.* **2020**, *21*, 6103.

[78] K. Tropmann, M. Bresinsky, L. Forster, D. Mönnich, A. Buschauer, H.-J. Wittmann, H. Hübner, P. Gmeiner, S. Pockes, A. Strasser, *J. Med. Chem.* **2021**, *64*, 8684–8709.

[79] E. Bartole, L. Grätz, T. Littmann, D. Wifling, U. Seibel, A. Buschauer, G. Bernhardt, *J. Med. Chem.* **2020**, *63*, 5297–5311.

[80] C. Ferrada, E. Moreno, V. Casadó, G. Bongers, A. Cortés, J. Mallol, E. I. Canela, R. Leurs, S. Ferré, C. Lluís, R. Franco, *Br. J. Pharmacol.* **2009**, *157*, 64–75.

[81] G. Navarro, D. O. Borroto-Escuela, K. Fuxe, R. Franco, *Neuropharmacology* **2016**, *104*, 161–168.